Hydrodynamic interface quench effects on spinodal decomposition for symmetric binary fluid mixtures

Hajime Tanaka
Institute of Industrial Science, University of Tokyo, Minato-ku, Tokyo 106, Japan
(Received 15 June 1994)

For nearly symmetric binary fluid mixtures, the coupling between concentration and velocity fields leads to a quick hydrodynamic coarsening. For bicontinuous phase separation, the pattern evolution is known to be governed by tube hydrodynamic instability. The interface tension is a driving force in the hydrodynamic coarsening. In the conventional theories of late-stage phase separation, local equilibrium has so far been assumed; however, this assumption might not be valid for nearly symmetric fluid mixtures even after the formation of a sharp interface. This is because the interfacial tension probably starts to play a major role in coarsening before the concentration reaches the local equilibrium concentration. In such a case, there is a possibility that the concentration diffusion cannot follow this quick geometrical coarsening. This could cause a drastic effect, which we call an *interface quench* effect. The *interface quench* effect could induce *spontaneous double phase separation* for bicontinuous morphology, especially under a geometrical confinement.

PACS number(s): 64.75.+g, 68.45.Gd, 68.10.−m, 05.70.Fh

I. INTRODUCTION

Phase-separation phenomena have been extensively studied by many researchers from both the experimental and the theoretical viewpoints [1,2]. The phenomena are commonly observed in mixtures of various types of condensed matter such as liquids, polymers, metals, semiconductors, and glasses. Phase-separation behavior in these types of condensed matters can be classified into a hydrodynamic group and a solid group, depending upon whether hydrodynamics plays a role in coarsening or not, respectively. In this paper, we focus our attention on unique features of the hydrodynamic group, which is widely known as the dynamic universality class *"model H"* in the Hohenberg-Halperin notation [3]. In the late stage of spinodal decomposition where a sharp interface is formed, the morphology of a phase-separated structure can be grouped into two types in terms of the composition symmetry: a bicontinuous structure for a nearly symmetric quench and a droplet structure for an off-symmetric quench. The typical phase-separation patterns (bicontinuous and droplet patterns) are schematically shown in Fig. 1. The coarsening mechanism for bicontinuous phase separation has been revealed to be the hydrodynamic coarsening driven by the capillary instability, which is known as Siggia's mechanism [4].

In the late stage, the local equilibrium has so far been assumed to be established and never to be broken for any mechanism [1,5–8]. Actually, all the coarsening mechanisms for the late-stage phase separation have been based on the local-equilibrium assumption or more precisely the fact that the compositions of both phases have their final equilibrium values [1]. This is the heart of the scaling concept for the late-stage phase separation. When the hydrodynamic coarsening plays an important role as in the case of the Siggia's mechanism [4], however, it is not obvious whether we can assume local equilibrium or not. In the late stage, the domain size R is much larger than the interface thickness, or the correlation length ξ, and in this regime it has been believed that the concentration is almost equal to the final equilibrium value and only the interfacial energy should be considered. This is obviously true for $R \gg \xi$, however, it is not clear how large the ratio R/ξ should be for the assumption to be valid. This assumption has been thought to be supported by the experimental fact of light scattering on phase-separating symmetric mixtures that the time exponent for the characteristic wave number q_m, α, and that for the scattering intensity maximum I_m, β, are connected as $\beta = 3\alpha$ [1,5–8]. In Fig. 8 of Ref. [5], for example, the quantity $q_m^3 I_m$ is roughly constant with time. Strictly speaking, however, it is an increasing function of time. This indicates that the concentration difference between two phases slightly increases with time for both isobutyric acid-water and 2,6-lutidine-water mixtures. Since the interfacial energy should be coupled with the local-equilibrium concentration through the requirement of the local free-energy minimum, we cannot neglect the dependence of the local-equilibrium concentration on the domain size [9–11] even for $R > 10\xi$. On the basis of this idea, we have recently proposed a concept of *"interface quench"* unique to a hydrodynamic group. The scaling relation $\beta = 3\alpha$ is not likely so sensitive to a slight deviation of the concentration from the final equilibrium one. Recent computer simulation of phase-separating binary fluids by Shinozaki and Oono [12] seems to support our idea since it indicates that the concentration does not necessarily reach its equilibrium value even after the formation of a sharp interface.

In this paper, we discuss effects of *interface quench* induced by the quick hydrodynamic reduction of the interfacial energy, which were proposed in previous papers [10,11]. Then, we demonstrate the importance of the coupling between the concentration and the velocity fields

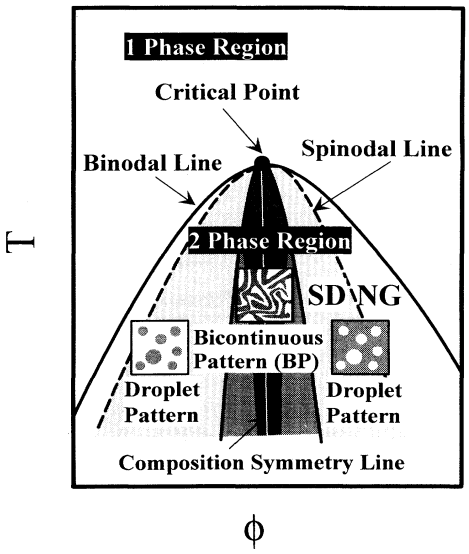

FIG. 1. A schematic phase diagram of a binary fluid mixture. The two-phase region is divided into metastable and unstable regions. In the former nucleation-growth-type phase separation (NG) occurs, while in the latter spinodal-decomposition-type phase separation (SD) occurs. From the morphological viewpoints, further, an unstable, spinodal region can be grouped into the two regions corresponding to bicontinuous phase separation and droplet phase separation, depending upon the composition symmetry. Here, we assume that the two components are dynamically symmetric for the sake of simplicity. The coarsening dynamics is closely correlated with the morphology. Any asymmetry breaks a bicontinuous structure and at a certain time there is a transition from a bicontinuous to droplet morphology. In the figure, the two bicontinuous regions are drawn for two different phase-separation times. The brighter region is for the earlier stage of phase separation, while the darker region is for the later stage.

due to the quick hydrodynamic coarsening for bicontinuous phase separation near a symmetric composition. The interface quench effect for droplet phase separation will be discussed in a forthcoming paper.

II. PHASE DIAGRAM

Before discussing the *interface quench effect*, the phase diagram for a typical binary mixture is discussed, focusing on the phase-separation morphology. It has been known that near the symmetric composition, bicontinuous phase separation proceeds. This bicontinuous phase separation could, however, be transformed into droplet phase separation by any asymmetry, such as the composition asymmetry [1] and the asymmetry in the viscoelastic property between the two phases [13–15]. The former has been well known and discussed by many researchers, while the latter has been largely unexplored. Dynamic asymmetry strongly affects both morphology and coarsening dynamics of phase separation and the behavior cannot be described by the conventional theories. Thus, in addition to the static composition symmetry, the dynamic symmetry reflecting the rheological properties of the separating phases should be considered [14,15]. Strictly, the conventional classification of morphology into bicontinuous and droplet patterns, which is based on the composition symmetry, is valid only for dynamically symmetric fluid mixtures. For the sake of simplicity, we consider only dynamically symmetric mixtures hereafter.

Here, we show a schematic phase diagram on morphology in Fig. 1. It should be stressed that whether a phase-separation morphology is bicontinuous-type or droplet-type is likely dependent on the phase-separation time and cannot be determined solely by the composition, as schematically shown in Fig. 1. A slight off-symmetry could lead to the morphological change from a bicontinuous to a dropletlike pattern (see, e.g., Fig. 1 in Ref. [16]). When the inside-outside symmetry is broken, the domains have a tendency to have a finite mean curvature and become spherical and, thus, a bicontinuous pattern could eventually transform into a droplet pattern. Only the exactly symmetric mixture could keep a bicontinuous morphology forever, if the other nonideal effects such as finite-size effects and gravity effects are negligible. Such an exactly symmetric situation might be realized only in a computer simulation. The percolation threshold for three dimensions has been believed to be $\Delta\phi \sim 1/3$, where $\Delta\phi$ is the deviation of the composition from the symmetric one normalized by the deviation of the equilibrium composition from the symmetric one. The region where bicontinuous phase separation is experimentally observed by optical microscopy, however, seems to be much narrower than this prediction (see Fig. 1 in Ref. [17]). We believe that this inconsistency between the percolation threshold theoretically estimated, and that experimentally determined is due to the invalid assumption of the random distribution of droplets in the theory. A droplet pattern has some regularity in its spatial distribution in spinodal decomposition, likely reflecting the conserved nature of the order parameter and also the nature of the coarsening due to a droplet collision [18]. This is natural since droplets always accompany the depletion layer, or the surrouding matrix. This regularity becomes weaker as the coarsening proceeds [18]. If we take into account the regularity of the spatial distribution of droplets, the percolation threshold of $\Delta\phi$ would be estimated to be much smaller than $\Delta\phi \sim 1/3$. Experimentally, there remains a slight possibility that this might be due to the fact that since optical microscopy observation can be applied only for the late stage, the crossover from a bicontinuous to droplet pattern could be finished before the structure becomes observable. We think, however, that the regularity in a droplet pattern is the more probable reason for the phenomenon observed than the nonideality of the experiments. Further experimental and theoretical studies on this problem is necessary. In this paper, we consider the hydrodynamic effect on bicontinuous phase separation, while in a forthcoming paper we will consider that on droplet phase separation.

III. EXPERIMENTAL EVIDENCE

Here, we briefly summarize experimental evidence indicating the effects of the hydrodynamic interface quench which were partly reported in Ref. [10].

A. Experiment

The samples used were mixtures of poly(vinyl methyl ether) (PVME) and water and mixtures of ϵ-caprolactone oligomer (OCL) and styrene oligomer (OS). For a PVME-water mixture, we used PVME having the weight-average molecular weight M_w of 98 200. In this mixture, the water-rich phase is more wettable to glass than the PVME-rich phase. The critical composition was PVME-water (7:93) and the critical temperature was 33.2 °C. The phase diagram of this mixture was shown in Fig. 1 of Ref. [17]. For an OCL-OS mixture, on the other hand, M_w of OCL and OS were 2000 and 1000, respectively. Polydispersity ratios of OCL and OS were 1.2 and 1.04, respectively. This mixture has an upper-critical-solution-temperature (UCST)-type phase diagram. The critical composition was OCL:OS(30:70) and the critical temperature was 135 °C. In this mixture, the OCL-rich phase is more wettable to glass than the OS-rich phase.

A sample mixture was set in a 1D capillary with the inner tube radius of r_0 or in a 2D capillary composed of two parallel plates with a gap of d. The thickness of glass plates for a 2D capillary was $\sim$ 100 μm. d was controlled by using monodisperse glass beads as spacers. The pattern evolution dynamics was directly observed in real space with video optical microscopy.

Phase separation in these mixtures was triggered by a temperature jump from the stable, one-phase region to the unstable, two-phase region. The temperature of a sample was changed by using a hot stage (Linkam TH-600RMS) typically with a rate of -3 °C/s. For a very deep quench beyond several degrees, we transferred a sample from one hot stage to the other hot stage. This method provides us with an extremely high quench rate. The phase-separation time was measured from the time when a sample starts to look cloudy, which roughly corresponds to the time when the temperature becomes the final one.

B. Double phase separation for bicontinuous phase separation in a confined geometry

Double phase separation (DPS) was observed in either one-dimensional (1D) or 2D capillaries under an influence of wetting [10]. Here, we demonstrate several examples of both usual phase separation and DPS under a geometrical confinement (see, also, Figs. 1 and 2 and their explanations in Ref. [10]).

Figure 2 shows phase-separation behavior of a PVME-water (7:93) mixture confined in a 1D capillary (r_0 = 200 μm) at 33.5 °C [17]. The quench depth ΔT was 0.3 °C. Since this composition was symmetric, bicontinuous phase separation was observed in the initial stage. Then the wetting layer is very quickly formed by the hydrodynamic instability unique to bicontinuous phase separation as already discussed in Ref. [17]. Then the wetting layer becomes unstable because of the Rayleigh-like instability and the tube configuration of the wetting layer is transformed into stable, periodic bridges (bamboolike structure). In the case of a shallow quench, we do not see any indication of double phase separation and each phase-separated phase is completely transparent.

Figure 3 shows pattern evolution of a PVME-water (7:93) mixture confined in a 1D capillary (r_0 = 79 μm) at 34.0 °C. The quench depth ΔT was 0.8 °C. Although the very initial stage of phase separation is similar to that in Fig. 2, the retarded, secondary phase separation was clearly observed inside the macroscopically separated phases in this case. This can be noticed around 1 s after the quench due to the fact that the two phases look cloudy. Then droplets caused by the secondary phase

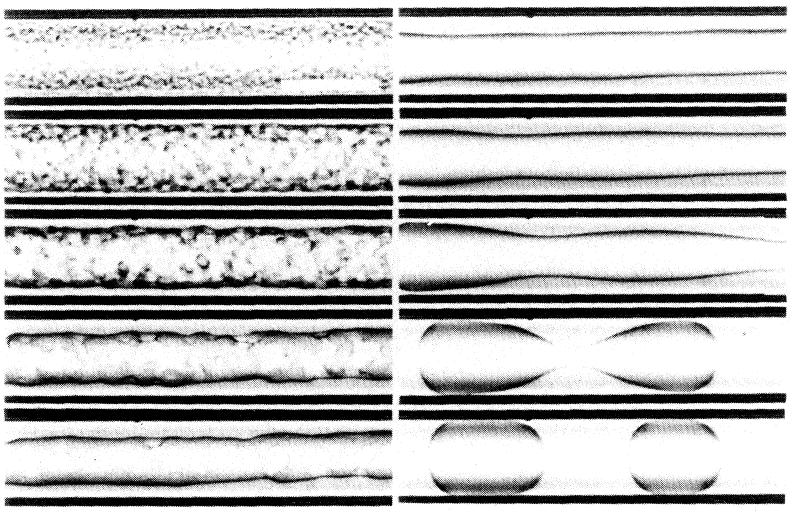

FIG. 2. Phase separation in a 1D capillary for PVME-water (7:93). Photographs correspond to 1.0 s, 1.5 s, 2.0 s, 3.0 s, 4.0 s (left column); 17.0 s, 57.0 s, 87.0 s, 127.0 s, 147.0 s (right column); from top to bottom, respectively, after the temperature jump from 32.5 °C to 33.5 °C. The bar corresponds to 200 μm.

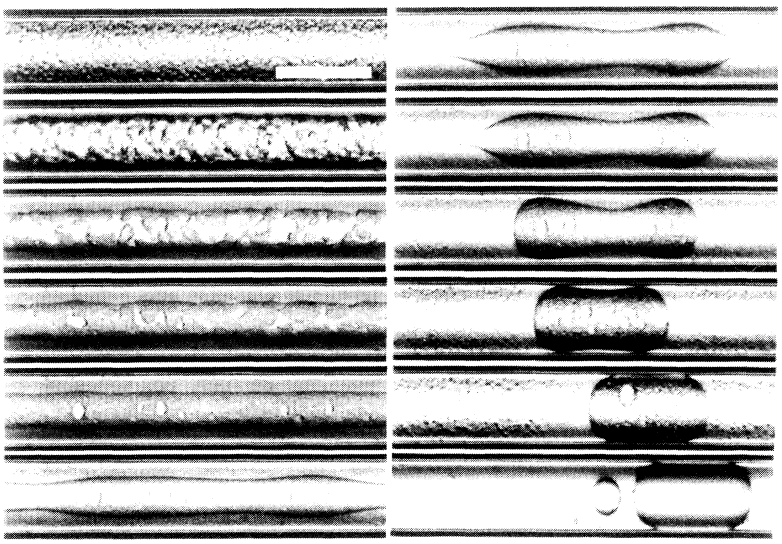

FIG. 3. Phase separation in a 1D capillary for PVME-water (7:93) mixture. Photographs correspond to 0.3 s, 0.8 s, 1.3 s, 1.8 s, 3.8 s, 16.8 s (left column); 22.3 s, 23.8 s, 28.8 s, 88.8 s, 479.0 s, and 3000 s (right column); from top to bottom, respectively, after the temperature jump from 32.5 °C to 34.0 °C. The bar corresponds to 200 μm.

separation grow to become visible around 20 s after the quench. This unusual phenomenon (DPS) was not observed for a shallow quench ($\Delta T \leq 0.6$ K) as shown in Fig. 2. It should be noted that only the essential difference between Figs. 2 and 3 is the quench depth.

Figure 4 shows phase-separation behavior of a PVME-water (10:90) mixture in a 1D capillary. In this particular case, we see double phase separation behavior only in one of the two phases (the polymer-rich phase). This unusual behavior is likely related to the slight asymmetry in composition; namely, only the polymer-rich phase becomes unstable while the water-rich phase does not [see the phase diagram (Fig. 1) in Ref. [17]].

Next, we show the results on 2D capillaries to understand the effects of the confinement geometry on the above phenomena (DPS). Figure 5 shows phase separation behavior of a PVME-water (7:93) mixture in a 2D capillary ($d \sim 3$ μm) at 33.3 °C. As in the cases of a 1D capillary, we do not see any double phase separation behavior for this quench condition. We see the pattern evolution unique to bicontinuous phase separation of symmetric fluid mixtures in a 2D capillary [9,19–21]. We see clearly the morphological transformation from an initial bicontinuous pattern in bulk to an assembly of disklike droplets connected via the wetting layer, and back to a 2D bicontinuous pattern. This transient appearance of droplet pattern is due to the fact that the in-plane symmetry of order parameter is broken by the wetting layer even for a symmetric mixture [21].

Figure 6 shows pattern evolution of PVME-water (7:93) in a 2D capillary ($d \sim 3$ μm) at 34.0 °C. It should be noted that only the difference in the experimental conditions between Figs. 3 and 6 is the confinement geometry. In the initial stage bicontinuous phase separation was observed. Then the wetting-induced domain ordering unique to a 2D capillary was observed [9,19]. Further, a retarded, secondary phase separation was observed as in a 1D capillary. It can be noticed around 1–2 s as a cloudy texture. Finally, the small droplets gradually disappeared by the evaporation-condensation mechanism as in the case of a temperature double quench [22]. Double phase separation was never observed for a shallow quench (see Fig. 5) as in the case of a 1D capillary.

Next, we show the results indicating the effects of the strength of the spatial confinement on DPS (see also Ref. [10]). Figures 7(a) and 7(b) show the d dependence of DPS for the same mixture confined in 2D capillaries with different gaps at the same temperature. It is found that DPS is severely suppressed by the strong spatial confinement as shown in Fig. 7(a): For a thick sample ($d \geq 3$ μm), DPS was clearly observed as in Fig. 7(b) and also in Fig. 6, while for a thin sample ($d < 1$ μm), it was never observed even though the other experimental conditions were the same. This fact indicates the importance of the bicontinuous phase separation in bulk.

To check whether or not the double phase separation is universally observed for any binary fluid mixtures, we also made similar experiments for OCL-OS mixtures (see also Ref. [10]). Figures 8 and 9 show similar examples observed in a mixture of OCL and OS. The composition was OCL:OS (3:7). As in the case of a PVME-water mixture, we observe the double phase-separation behavior. The phase separation is characterized by the existence of small droplets of the complementary phase in both phases.

Finally, we show that this phenomena of double phase separation is observed only for bicontinuous phase-separation and it has never been observed for droplet phase separation. Figure 10 shows the phase-separation behavior in an OCL-OS (5:5) mixture which is an off-symmetric mixture, at 60 °C. Although the quench condition was about the same as the cases of the symmetric composition, double phase separation was never observed for droplet phase separation. This fact was quite general and we have never seen double phase separation under all the experimental conditions studied for any binary fluid mixtures including PVME-water mixtures (see, e.g., Figs. 2 (a) and 2(b) in Ref. [17]).

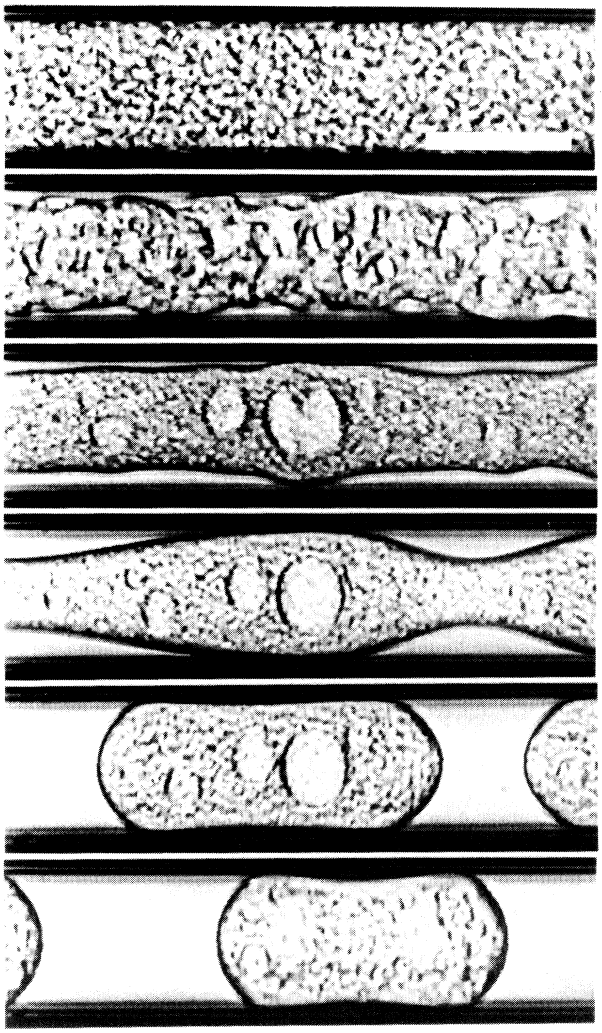

FIG. 4. Phase separation in a 1D capillary for PVME-water (10:90). Photographs correspond to 0.5 s, 1.0 s, 2.0 s, 18.0 s, 28.0 s, and 238.0 s, from top to bottom, respectively, after the temperature jump from 32.5 °C to 34.1 °C. The bar corresponds to 80 μm. In this case, the composition slightly deviates from the symmetric one (7:93). Double phase separation is selectively observed only in the polymer-rich (less-wettable) phase.

IV. INTERPRETATION OF THE PHENOMENA BASED ON THE CONVENTIONAL MECHANISMS

A. Usual mechanisms of bulk phase separation

The similar phenomena have also been reported by Wiltzius and Cumming [23], Cumming *et al.* [24], and Guenoun *et al.* [25]. These phenomena, however, have not been seriously discussed. They have so far been interpreted by usual bulk phase separation [23,24,26,27] or by the disconnection of some domains during the growth of the percolated pattern [25]. As reported in Refs. [9,10], however, we think that the phenomenon is caused by the *interface quench* effect. We can clearly see the homogeneous appearance of small droplets in both phases as in the usual phase separation (see Figs. 3, 4, and 6–9 in this paper and also Figs. 1–3 in Ref. [10]). Further, the double phase separation is not observed for a small ΔT. These facts are explained by neither usual bulk phase separation nor the disconnection of some domains from the bicontinuous tubes. Since the latter phenomenon (the breakup of the tubes) is likely caused by the asymmetry in the composition and/or in the viscoelastic property between the two phases, it is rather difficult to expect the symmetric situation that small droplets of the complementary phase appear in both macroscopic phases. Further, a rather uniform size of small droplets indicates that the phenomenon is not caused by the breakup of tubes since it could occur sequentially at any time and should produce various sizes of droplets. More importantly, this mechanism cannot explain the asymmetric situation in Fig. 4 that only one of the two phases undergoes double phase separation. This secondary phase separation always has a droplet morphology even for a symmetric quench, strongly indicating that this is not usual bulk phase separation and is caused by a *double quench effect* for the two macroscopically separated phases. As will be described later, the above behavior can be explained by the *interface quench* effect [9,10] induced by the quick reduction of the total interface area, which is equivalent to a temperature double quench [22]: Both compositions of the two original phases just before the *interface quench* ($\sim \pm\Delta\phi_t$) are off-critical and strongly asymmetric in composition [22]. Further, the slow coarsening is consistent with the fact that the secondary temperature quench depth (δT) which is equivalent to the *interface quench* (see Ref. [10] and the discussion in Sec. VI) is shallow.

B. Solid-surface effect

Another possibility is a solid-surface effect [10]: The quick reduction of the solid-liquid interface energy caused by the wetting layer formation might lead to the quick change in the total free energy. This should not, however, be the case because of the following reasons. (i) The effect should be more important near the critical point since the relative importance of the solid-liquid interface energy ($\propto (\Delta T)^{0.34}$) against the bulk excess energy which is dominated by the liquid-liquid interface energy ($\propto (\Delta T)^{1.26}$) decreases with the quench depth ΔT. This is inconsistent with the fact that DPS is observed only for a deep quench. (ii) The behavior is completely similar between Figs. 3 and 6, although the surface:volume ratio is so different between them. Further, DPS is suppressed by a strong spatial confinement (see Fig. 7 and Ref. [10]), where the solid-surface energy should play a more important role than for a thick sample. This denies the possibility of a solid-surface effect and rather indicates the importance of the bulk hydrodynamic process for DPS. Marko has recently explained the reason why the $t^{1/3}$-law bulk growth is observed in Refs. [23,24], as follows: The

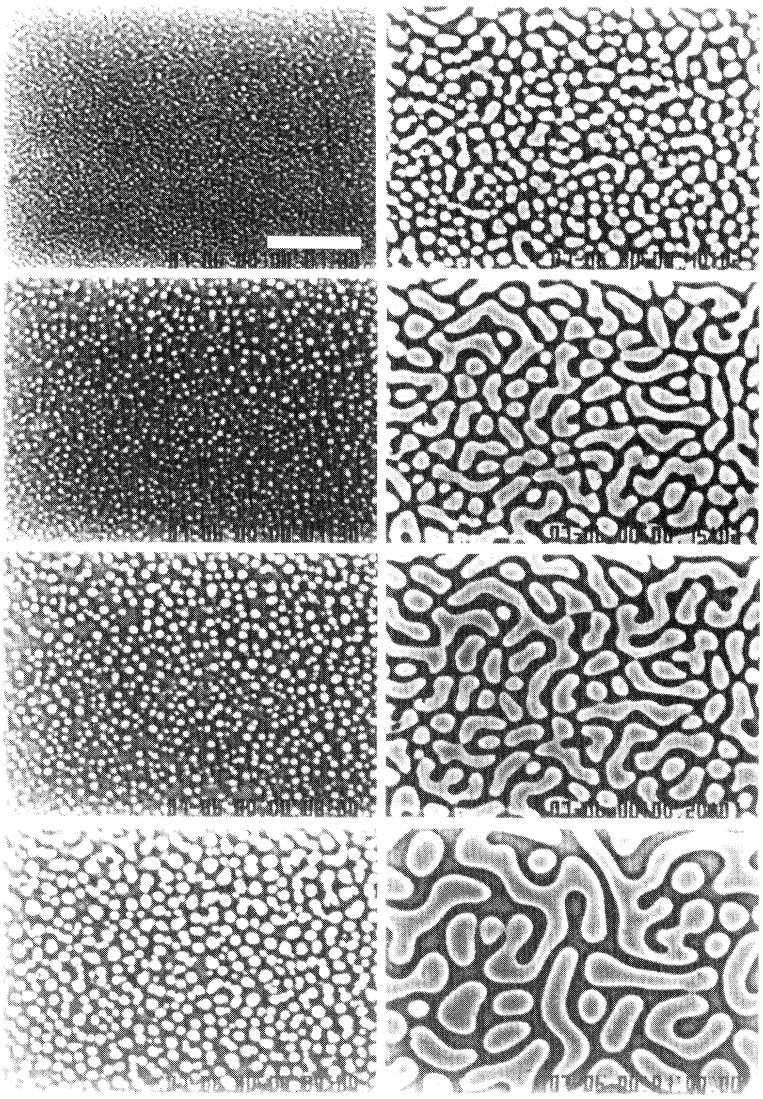

FIG. 5. Phase separation in a 2D capillary ($d \sim 3$ μm) for PVME-water (7:93). Photographs correspond to 1 s, 1.5 s, 2 s, 3 s (left column); 4 s, 9 s, 14 s, and 54 s (right column); from top to bottom, respectively, after the temperature jump from 32.5 °C to 33.3 °C. The bar corresponds to 80 μm.

imbalance composition induced by the surface is sufficient to disconnect domains so that hydrodynamic coarsening cannot proceed. This mechanism could be important for a binary mixture confined in a microscopic pore. In our case, however, it can probably be denied by the same reasons as those for the above solid-surface effect.

C. Thermal history effects

Next, we discuss the possibility that the phenomena might be caused by a nonideal temperature quench. For the quench of $\Delta T = 1$ K the sample temperature was settled within 1 s to the final one (± 0.1 K) for a sample thickness of 20 μm, which was experimentally confirmed by a direct measurement of a sample temperature using a thin thermocouple [10]. The result is shown in Fig. 11. The temperature-change process during the quench can be regarded as a sharp steplike function. For polymer solutions and polymer mixtures, the characteristic diffusion time is much longer than for simple fluid mixtures. Thus, this quench speed could be regarded as an instantaneous quench. Further, the experimental results by Cumming *et al.* [24] indicate that DPS is not due to an artifact of a noninstantaneous quench: The secondary phase separation starts to be observable by light scattering around 3×10^3 s for their shallowest quench of $\Delta T = 0.15$ K (see Fig. 13 in Ref. [24]), sufficiently after the complete stabilization of the temperature which takes ~ 50 s (see Fig. 4 in Ref. [24]). In the light of the current understanding of the thermal history effect, it could be said that DPS is free from a noninstantaneous quench effect.

At a present stage, however, we cannot clearly determine whether a certain quench speed is fast enough or not, to deny the possibility that double phase separation is caused by the thermal history effects, since there is no clear criterion about this problem. Thus, we need additional strong evidence to support that the double phase separation is intrinsically caused by the *spontaneous interface quench*, and not by the thermal history effects.

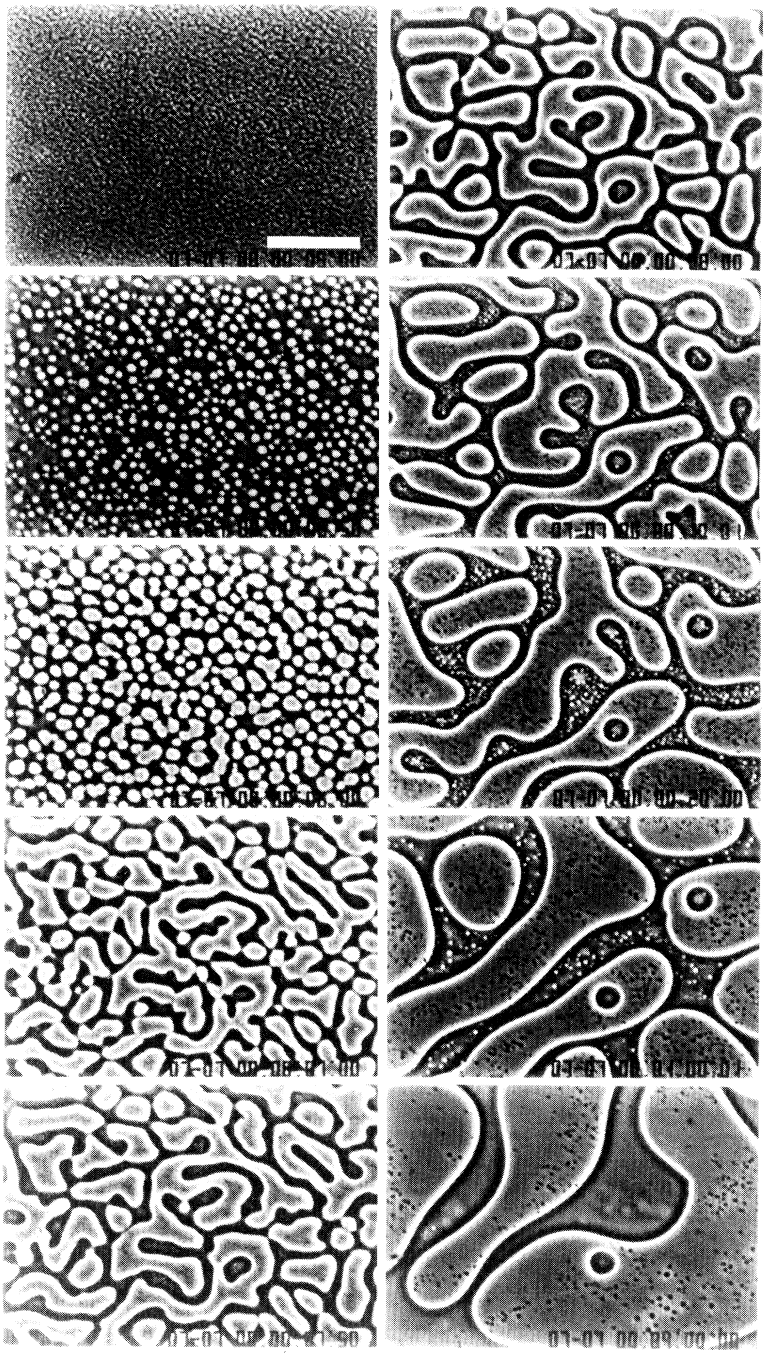

FIG. 6. Phase separation in a 2D capillary ($d \sim 3$ μm) for PVME-water (7:93). Photographs correspond to 0.2 s, 0.7 s, 1.2 s, 2.2 s, 2.7 s (left column); 3.2 s, 5.2 s, 15.2 s, 55 s, and 235 s (right column); from top to bottom, respectively, after the temperature jump from 32.5 °C to 34.0 °C. The bar corresponds to 80 μm.

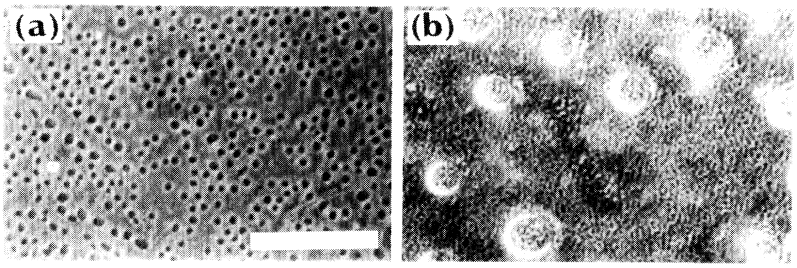

FIG. 7. Phase-separation behavior in a 2D capillary for PVME-water (7:93) at 34.0 °C. Both photographs were taken at 20 s after the temperature jump from 32.5 °C to 34.0 °C. (a) $d \sim 1$ μm, (b) $d = 15$ μm. In (b), the coexistence of large and small domains is seen, while not in (a). The bar corresponds to 100 μm.

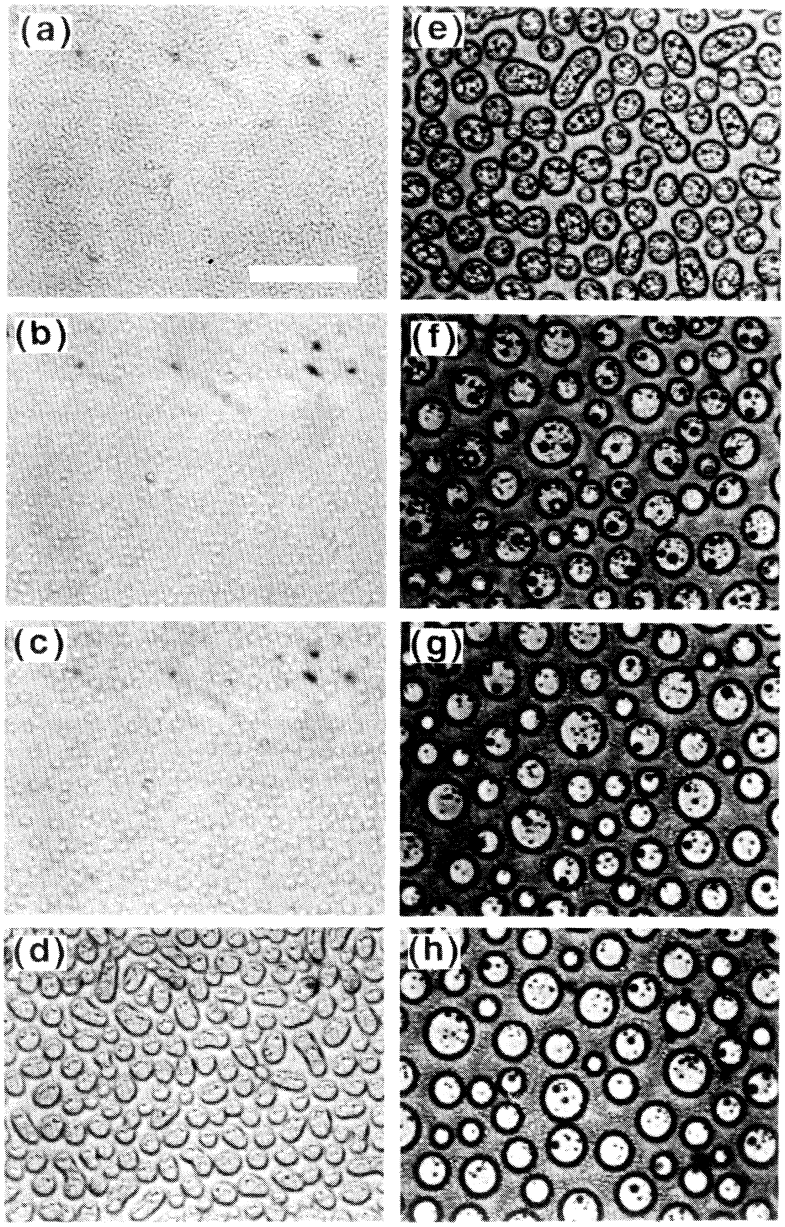

FIG. 8. Double phase separation observed in an OCL-OS (3:7) mixture at 60 °C. We can clearly see the secondary phase separation. The sample thickness d is about 8 μm. (a) 0.8 s, (b) 1.2 s, (c) 1.4 s, (d) 2 s, (e) 6 s, (f) 111 s, (g) 590 s, (h) 1200 s after the quench. The bar corresponds to 100 μm.

For samples having the same thermal history, double phase separation was observed only for nearly symmetric mixtures showing bicontinuous phase separation where the coarsening is hydrodynamically driven by capillary instability. It should be stressed that double phase separation was never observed for off-symmetric mixtures having a droplet morphology. This fact can easily be confirmed by comparing Fig. 3 in this paper and Figs. 2(a) and 2(b) in Ref. [17] together with the phase diagram (Fig. 1 in Ref. [17]) and also by comparing Figs. 8 and 10 in this paper. We have checked many cases for different compositions and different quench depths and found that this fact is quite general. Further, we have confirmed that double phase separation is not observed for droplet phase separation in OCL-OS (5:5) mixture even for a slow temperature quench which takes 60 s for the quench $\Delta T = 30$ K. This quench rate is more than 10 times slower than that in Figs. 8, 9, and 10. This indicates that even a very slow quench does not cause double phase separation for droplet phase separation, although a much slower quench would, of course, lead to DPS caused by thermal history effects [22].

The *interface quench* effect is likely caused only by the special hydrodynamics unique to a bicontinuous pattern. Thus, the secondary phase separation should not occur at asymmetric compositions since there the minority phase forms droplets, everything is governed by diffusion phenomena, and the reduction of the interface area is so slow: The local equilibrium is not severely violated in droplet phase separation at asymmetric compositions. This is consistent with our experimental results. The same behavior dependent on a phase-separation morphology was

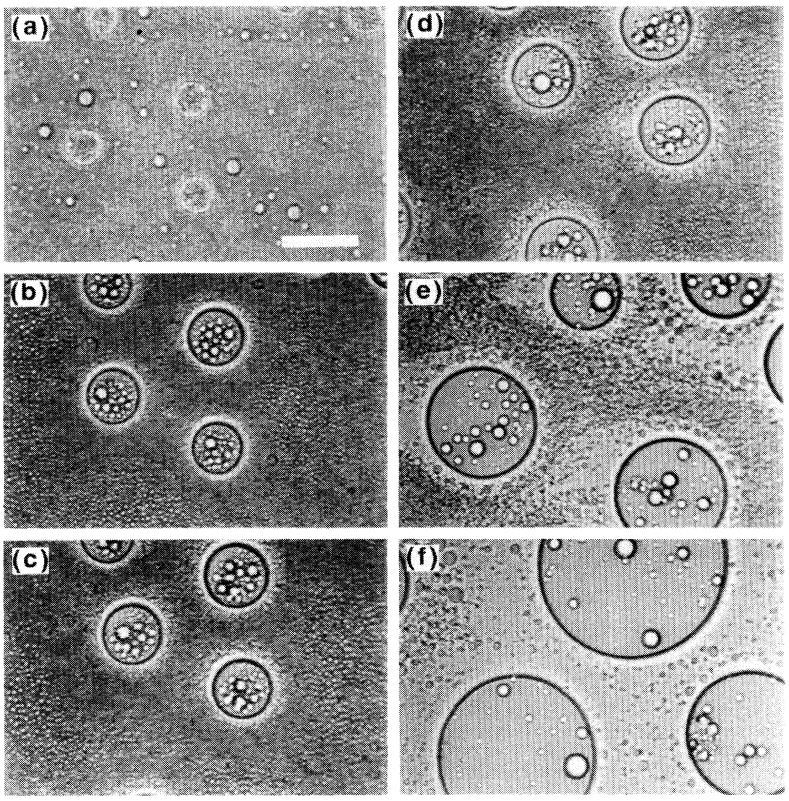

FIG. 9. Double phase separation observed in OCL-OS (3:7) at 100 ° C. We can clearly see the secondary phase separation. The sample thickness d is about 53 μm. (a) 7 s, (b) 21 s, (c) 39 s, (d) 64 s, (e) 183 s, (f) 603 s after the quench. The bar corresponds to 100 μm.

observed in other binary mixtures such as polystyrene (PS)-PVME mixtures, and low molecular dye-PS mixtures. This fact could be strong evidence that the double phase separation is not caused by thermal history effects and it is intrinsically induced by the *interface quench effect unique to symmetric fluid mixtures.* It should be noted that there remains a slight possibility that the effect of a finite quench speed might be significant only for fast bicontinuous phase-separation and not for slow droplet phase separation: The saturation of the concentration to the equilibrium value is likely faster in bicontinuous phase separation than in droplet phase separation simply because the coarsening speed is higher in the former than in the latter. This difference between the two types of phase separations could play a role in producing thermal history effects only for a slow quench, where the temperature changes even after the formation of a sharp interface (see the discussion below).

Relating to the existence of DPS only for bicontinuous phase separation, we check here the possibility of thermal history effects from another aspect. In the current understanding of the phase-separation dynamics [1,28], the difference in coarsening behavior between bicontinuous and droplet phase separation can be schematically summarized as shown in Fig. 12. In the scaled plot, the coarsening behavior is basically the same between the two types of phase separation for both the initial linear regime and the slow coarsening regime affected by nonlinearity. Only the difference is caused by the fact that the hydrodynamic coarsening mechanism works selectively for bicontinuous phase separation after the formation of a sharp interface. Thus, if a nonideal behavior of the temperature change is localized in the time region of the early (linear) stage and the subsequent slow coarsening stage (the shaded region in Fig. 12), there should be no essential difference in the thermal history effects between bicontinuous and droplet phase separation. This means that the concentration distribution should be the same between them, and accordingly the stability of the two phases should also be the same between them. The quench conditions of Wiltzius and Cumming [23] likely satisfy the above requirement that the transient process of the temperature quench is localized in the time region of the early stage. This also suggests that DPS is not caused by the thermal history effects. Even in such a case, however, we cannot completely deny the possibility that thermal history effects appear differently between droplet and bicontinuous phase separation: There remains the possibility that the modification in the concentration distribution function due to thermal history effects in the early stage could develop with time in a different way between the two types of phase separation in the late stage.

The quench speed which is partly dominated by a thermal conduction should be slower for the 1D capillaries ($d \sim 100 - 200$ μm) than for the 2D capillaries ($d \sim 2 - 100$ μm). We have never notice any essential difference in the occurrence of DPS between the two cases for the mixtures of PVME and water. This fact also seems to support that DPS is an intrinsic phenomenon which is not caused by a nonideal thermal quench.

Further strong evidence that DPS is not caused by

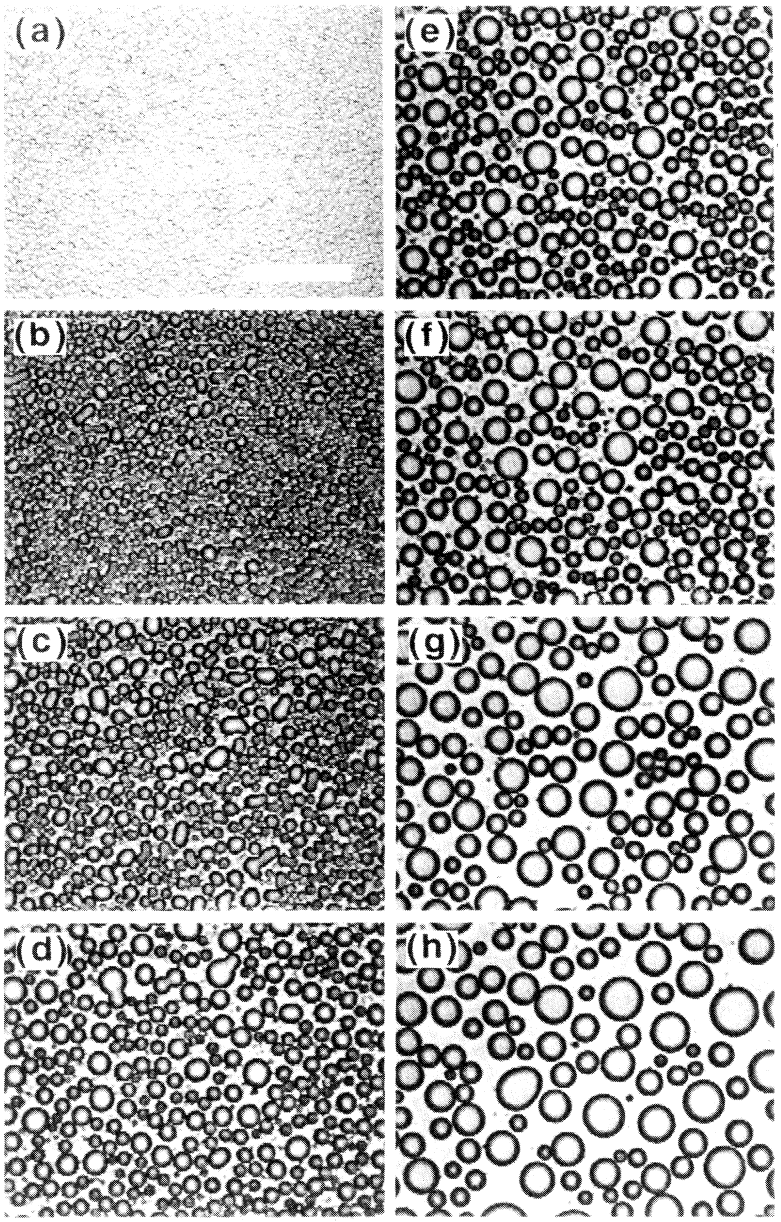

FIG. 10. Phase separation in a 2D capillary for OCL-OS (5:5) at 60 °C. The quench depth and the quench rate are the same as those in Fig. 8. The sample thickness d is about 8 μm. (a) 5 s, (b) 10 s, (c) 20 s, (d) 60 s, (e) 240 s, (f) 540 s, (g) 1740 s, (h) 2940 s after the quench. Here, there is no indication of secondary phase separation. The bar corresponds to 100 μm.

thermal history effects is that DPS is not observed in a very strong geometrical confinement (see Fig. 7 and Ref. [10]) [29]. Since the characteristic thermal diffusion time is roughly 1 ms even for a length scale of ~ 10 μm, the quench time is largely dominated by the characteristic thermal time determined by the hot stage and the cell wall (~ 1 s in our case). This means that the difference in the sample thickness between 1 μm and 3 μm would not cause any significant difference in the quench speed. This is also supported by the similarity of the phenomena between the thick 1D capillaries and the thin 2D capillaries. Thus, the suppression of DPS by a strong confinement cannot be explained by thermal history effects. It could be explained by the suppression of bulk hydrodynamic coarsening due to the geometrical confinement: Under a strong geometrical confinement the interface area of a system cannot be drastically reduced because of the dimensional crossover in the rather early stage of phase separation and the resulting slowing down of coarsening.

Finally, it should be noted that this problem of thermal history effects is the most crucial and naive experimental problem relating to DPS. Although we have many indications which strongly suggest that DPS is not caused by a thermal history effect, it is necessary to completely deny this possibility in a more direct way to conclude that DPS is a real intrinsic phenomenon. Thus, we need to continue to make careful studies on this problem. Numerical simulations seem to be most promising since experimentally it is very difficult to realize a very quick deep quench. The fastest quench is likely a pressure quench. It intrinsically includes the two effects, dT_c/dP and $(\partial T/\partial P)_S$, however. The latter effect, namely, the adiabatic tem-

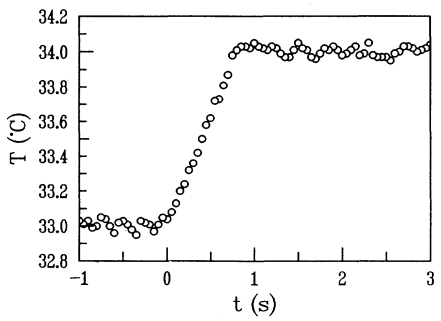

FIG. 11. Temporal change in the temperature of a sample during a typical quench process. The time $t = 0$ corresponds to the beginning of the temperature jump.

perature change, often complicates the thermal behavior of a sample since a sample is usually under an isothermal condition. This itself could even lead to a double temperature quench. An electrical-field quench is another candidate of a quick quench, although it introduces the anisotropy in an isotropic sample.

The double phase separation phenomena have been observed for both upper-critical-solution-temperature (UCST) type (OCL-OS mixtures) and lower-critical-solution-temperature (LCST) type phase diagrams (PVME-water and PS-PVME mixtures). Thus the phenomena cannot be explained by any other thermal reasons such as the temperature change induced by the latent heat release during the phase separation.

V. THEORETICAL BACKGROUND

Before discussing a new mechanism, it is noteworthy to point out the essential difference between solid and

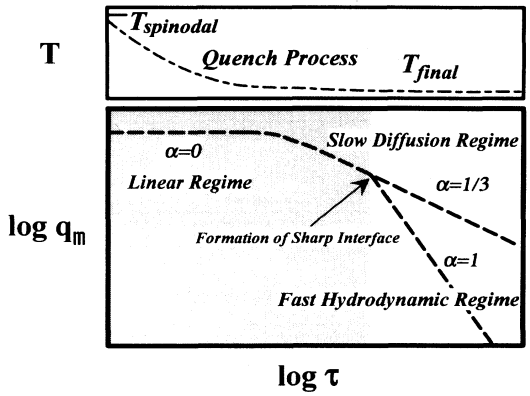

FIG. 12. A schematic figure of the coarsening behavior for both bicontinuous and droplet phase separation. In both cases, diffusion dominates the coarsening behavior until the formation of a sharp interface. The shaded region is the time regime dominated by concentration diffusion. Here, α is the time exponent of the scaling relation $q_m \sim t^{-\alpha}$. If the transient process of a temperature quench is localized only in the shaded region, the thermal history effects should affect the phase separation in the same way for both types of phase separation.

fluid systems: For a solid system the gross variable is only the composition ϕ, while for a fluid system they are ϕ and the velocity field $\vec{v}$. Thus, the kinetic equations for classical binary fluids are [1]

$$\frac{\partial \phi}{\partial t} = -\vec{\nabla} \cdot (\phi \vec{v}) + L_0 \vec{\nabla}^2 \frac{\delta F}{\delta \phi} + \theta, \tag{1}$$

$$\rho \frac{\partial \vec{v}}{\partial t} = -\vec{\nabla} \cdot \mathbf{\Pi} - \vec{\nabla} p_1 + \eta \vec{\nabla}^2 \vec{v} + \vec{\zeta}, \tag{2}$$

$$F = \int d\vec{r} \left[-\frac{r}{2}\phi^2 + \frac{u}{4}\phi^4 + \frac{K}{2}(\vec{\nabla}\phi)^2 \right]. \tag{3}$$

Here, $\mathbf{\Pi}$ is the stress tensor caused by the fluctuation of ϕ. ρ is the density, p_1 is a part of the pressure, and η is the viscosity. Here, we assume the viscosity is the same for the two component fluids. θ and $\vec{\zeta}$ are random forces. The first term of the right-hand side of Eq. (1) is the streaming term. The characteristic feature of the fluid system is that the velocity field $\vec{v}(\vec{r}, t)$ strongly affects the dynamics.

In the late stage where the sharp domain boundary is formed, $-\vec{\nabla} \cdot \Pi = -\phi \vec{\nabla}(\delta F/\delta \phi)$ can be given by [30]

$$-\vec{\nabla} \cdot \mathbf{\Pi} = -\vec{\nabla}(\phi \delta F/\delta \phi) + k_B T (1/R_1 + 1/R_2)(\partial \phi_{\rm int}/\partial \zeta)^2 \vec{n}.$$

Further $(\partial \phi_{\rm int}/\partial \zeta)^2$ can be approximated by $\delta(\zeta)$. Provided that the velocity field is slowly changing following the domain and thus $\partial \vec{v}/\partial t \sim \vec{0}$, Eq. (2) becomes as follows:

$$-\vec{\nabla} p_1 + \sigma (1/R_1 + 1/R_2)\delta(\zeta)\vec{n} + \eta \vec{\nabla}^2 \vec{v} \sim \vec{0}.$$

For a bicontinuous morphology, the solution is given by

$$v_i(\vec{r}) \sim \int da \Sigma_j T_{ij}(\vec{r} - \vec{r}_a) \sigma \left(\frac{1}{R_1} + \frac{1}{R_2} \right)_a n_j(\vec{r}_a) \,,$$

$$T_{ij} = \frac{1}{8\pi\eta} \left(\frac{\delta_{ij}}{r} + \frac{x_i x_j}{r^3} \right).$$

Here, $T_{ij}(\vec{r})$ is the so-called Oseen tensor, $\vec{r}_a$ is the point on the interface, and da is the area unit. $(1/R_1 + 1/R_2)_a$ is the curvature at $\vec{r}_a$.

From the above consideration, the characteristic velocity field is estimated as σ/η. This velocity field is regarded as the same as the interface velocity and, thus, $v_n = \vec{n} \cdot \vec{v} \sim \partial R/\partial t$. Accordingly, we obtain the Siggia's growth law, $R(t) \sim (\sigma/\eta)t$.

In the above discussion, the velocity field is treated as being independent of the concentration field and Eq.(2) is independently solved. Thus, the hydrodynamic effect is not considered through $\vec{v}$ on the basis of Eq. (1). This is based on the assumption that in the late stage, the concentration reaches the equilibrium value and only the interface contributes the free energy of the system, which leads to $\partial \phi/\partial t \sim 0$. This assumption might not, however, be valid in the intermediate stage as will be explained later. For a hydrodynamic system, there is a streaming term, $\vec{\nabla} \cdot (\phi \vec{v})$, in the diffusion equation and the situation is probably not that simple. This coupling between the velocity and concentration fields could cause an additional hydrodynamic effect on spinodal decomposition.

VI. CONTINUOUS INTERFACE QUENCH IN BICONTINUOUS PHASE SEPARATION

A. Bulk phase separation

1. Concept of interface quench

In bicontinuous phase separation, the total interface area of the system is drastically reduced within a short time by the hydrodynamic coarsening originating from the coupling between the concentration and the velocity fields. According to the Siggia's mechanism [4], the interface area per unit volume s is estimated to decrease as $s = [k(\sigma/\eta)t]^{-1}$, where σ is the interface tension, η is the viscosity, and k is a constant. Since the interface motion caused by the tube hydrodynamic instability is much faster than the concentration diffusion, the hydrodynamic flow due to the capillary instability causes only the geometrical coarsening and does not accompany the concentration change by itself. Thus, the system cannot respond to the rapid decrease in the interface energy. This likely causes a kind of double quench effect. Here, we call this phenomenon *interface quench* [9,10]. In all the previous studies [1], the local-equilibrium has been assumed in the so-called late stage where the hydrodynamic effect plays a role in coarsening, but it is probably not true in the exact sense. Namely, the local-equilibrium assumption could be violated by the coupling between the concentration and the velocity fields. The hydrodynamics starts to play a role after the establishment of a sharp interface, namely, after the characteristic size of phase separation R exceeds the correlation length (or the interface thickness) ξ. Even without the change in the concentration, the total free energy could be lowered by the reduction of the interface area since the hydrodynamic process is much faster than the diffusion process.

Related to the above physical picture, there remains a slight question as to whether this phase-separation behavior is a unique solution for hydrodynamic systems or not: For example, is it possible that the retardation of diffusion might slow down the hydrodynamic coarsening itself to prevent secondary phase separation? Presently, however, we think that such a possibility is low for the following reason: The interface motion is described by Eq. (2). The diffusion flow due to the concentration deviation from the local-equilibrium one apparently plays negligible roles in the interface motion compared to the hydrodynamic flow due to capillary instability after the formation of a sharp interface. It should be noted that these two effects have entirely different physical origins and they are mostly independent with each other. In the early stage the diffusion plays a very important role in coarsening, but it becomes weaker as the concentration approaches to the local-equilibrium one. In the late stage where a sharp interface is formed, on the other hand, the hydrodynamic flow plays a dominant role.

2. Estimation of interface quench effect

For a bulk symmetric mixture, it is well known that the phase separation is dominated by the hydrodynamics unique to a bicontinuous pattern and the pattern coarsens as $R = k_b(\sigma/\eta)t$ (R: the characteristic domain size) in the late stage [1,4,31]. For bicontinuous phase separation, the tube flow is essentially caused by the fluctuation of a tube diameter. Siggia estimated k_b as 0.1 on the basis that the pressure difference along the tube is $\sim \sigma/R$ [4]. As pointed out by Siggia [4], this pressure difference is probably overestimated for the tube-radius fluctuation. Wong and Knobler [32] estimated k_b as 0.001 from their experimental results. San Miguel *et al.* [33] theoretically reestimated k_b on the basis of the capillary instability and they obtained the relation $k_b \sim 0.04$ for the two-phase fluids having similar viscosity. The recent experiments by Guenoun *et al.* [25] and by Bates and Wiltzius [8] supported this evaluation ($k_b \sim 0.04$). Thus, we employ $k_b \sim 0.04$ in the following.

The effect of the *interface quench* can be estimated as follows. After the formation of a sharp interface (the domain size $R >$ the interface thickness ξ), we can assume from the scaling concept, the statistical property of the interfacial pattern does not change in time and the pattern is self-similar. This idea that focuses only on the interface dynamics was first introduced theoretically by Kawasaki and Ohta [30] to simplify the late-stage coarsening dynamics. By introducing the time dependence of $\Delta\phi$, this could be more generalized as

$$\phi(\vec{r},t) = \Delta\phi(t) H(R(t)\vec{r}), \tag{4}$$

on the crude assumption of the independence between $\Delta\phi(t)$ and $R(t)$. Further, we should note important points to solve the problem: (1) The temporal change in $\Delta\phi$ needs the diffusion process because of the conservation law. (2)The growth of the interfacial pattern is a hydrodynamic process, and should be fast. The evolution of the interface pattern is almost purely described by the hydrodynamics, namely, by Navier-Stokes equation [Eq.(2)] [30]. The interface velocity is obtained from Eq. (2) as $v_n \sim \sigma/\eta$. Using the fact that $\Delta\phi(t)$ is the slowly varying variable and assuming an exactly self-similar growth, we get

$$\vec{\nabla}\phi \sim \vec{n}(a)\Delta\phi\partial H(R(t)\vec{r})/\partial n\ , \tag{5}$$

$$\partial\phi/\partial t \sim -v(a)\Delta\phi\partial H(R(t)\vec{r})/\partial n + H(R(t)\vec{r})\partial\Delta\phi/\partial t. \tag{6}$$

Here, $\vec{n}(a)$ is the unit vector normal to the interface at a and $v(a)$ is the speed of the interface a along $\vec{n}(a)$. Here, $\partial H(R(t)\vec{r})/\partial n$ is similar to δ function which is nonzero only around the interface. It should be noted that the exact self-similarity assumed above is rather unrealistic and the self-similarity holds only statistically. Using these relations, Eq. (1) becomes

$$H(R(t)\vec{r})\partial\Delta\phi/\partial t \sim L_0\nabla^2\delta F(\Delta\phi)/\delta\Delta\phi. \tag{7}$$

The assumptions made here are as follows: (i) The coarsening is dominated purely by hydrodynamics and the velocity field is determined by Eq. (2) independently from $\Delta\phi(t)$ and (ii) the averaged order parameter $\Delta\phi$ tries to

follow the local-equilibrium determined by the geometrical coarsening. Since it is rather difficult to argue the stability of the phase in a straightforward manner, we will discuss the problem on the basis of the local-equilibrium relation $\delta F/\delta\Delta\phi \sim 0$. This is a crude approximation, but should give us a good starting point for understanding the interface quench effect. It should be noted that this local-equilibrium assumption gives us the fastest change in the local-equilibrium concentration caused by coarsening. The stability of the phase will be studied with the constraint that the system geometrically coarsens with time by tube hydrodynamic instability as $R \propto t$.

Provided that the concentration profile can be approximated by a trapezoidal-like shape with an interface width of ξ [34] ($\xi \ll R$) for the sake of simplicity,

$$F(\Delta\phi) = \left[-\frac{r}{2}(\Delta\phi)^2 + \frac{u}{4}(\Delta\phi)^4\right] V_d R^{d_p} + \frac{K}{2}\left(\frac{\Delta\phi}{\xi}\right)^2 \xi S_d R^{d_p-1}, \quad (8)$$

where $\Delta\phi$ is the concentration of the phase measured from the average one, d_p is the effective dimensionality of the pattern, and S_d and V_d are the surface and volume prefactors, respectively (e.g., $S_d = 4\pi$ and $V_d = 4\pi/3$ for a 3D sphere). Here, we assume $d_p \sim S_d/V_d \sim 1$ for a bicontinuous pattern. It should be noted that the result is likely insensitive to the details of the concentration profile at the interface. Further, we assume that the interface thickness is constant with time in the late stage and equal to ξ. Then we can estimate the local-equilibrium concentration $\Delta\phi_l$ for a domain size of R from the local energy minimum condition as follows

$$\Delta\phi_l^2 = \left(r - \frac{K}{\xi R}\right)/u,$$
$$\Delta\phi_l = \Delta\phi_b\left(1 - \frac{K}{\xi R r}\right)^{1/2} = \Delta\phi_b\left(1 - \frac{2\xi}{R}\right)^{1/2}, \quad (9)$$

where $\Delta\phi_b = (r/u)^{1/2}$ is the final equilibrium concentration for an infinite domain size and gives the binodal line. Here, the relation $\xi^2 = K/2r$ is used. The spinodal line is given by $\pm\Delta\phi_s = (r/3u)^{1/2}$. Figure 13 shows the dependence of $\Delta\phi_l/\Delta\phi_b$ on R/ξ, based on Eq. (9). It should be noted here that Eq. (9) is likely invalid for a small value of R/ξ. Since r is proportional to the quench depth ΔT, the jump of $(-1/R)$ has the same meaning as the jump of ΔT, according to Eq. (9). Using the relation $\Delta\phi_b = m\Delta T^\beta$ ($\beta \sim 0.33$, m: a constant), the transient ΔT (ΔT_t) which satisfies $\Delta\phi_b(\Delta T_t) = \Delta\phi_l(\Delta T, R_t)$, is estimated as

$$\Delta T_t = \Delta T\left(1 - \frac{2\xi}{R_t}\right)^{1/2\beta}, \quad (10)$$

where it is assumed that at $R = R_t$ the interface quench is initiated. Thus, the *interface quench* caused by the hydrodynamic coarsening from small domains ($R_t \geq \xi$) to large domains ($R >> \xi$) is equivalent to the temperature double quench [22] composed of a first quench (ΔT_t) and a second deeper quench ($\delta T = \Delta T - \Delta T_t$). Thus it is

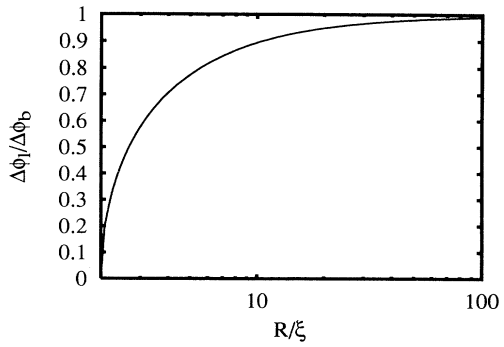

FIG. 13. A schematic figure explaining the dependence of $\Delta\phi_l/\Delta\phi_b$ on R/ξ for bicontinuous phase separation [see Eq. (9)].

expected that the two, macroscopically separated phases become unstable or metastable by the *interface quench effect*. For example, δT is estimated as 0.3 ΔT and 0.03 ΔT for $R_t \sim 10\xi$ and $R_t \sim 100\xi$, respectively. Thus, the *interface quench* should have a significant double quench effect.

To check the above possibility, we have to study whether the concentration diffusion can follow this quick change in the local-equilibrium concentration from $\Delta\phi_t$ to $\Delta\phi_b$ and whether the local equilibrium can be established within the time scale of hydrodynamic coarsening, or not. The time required to hydrodynamically form the macroscopic phase having a domain size R is estimated as $\tau_h \sim (R - R_0)\eta/(k\sigma)$. Here, R_0 is the size of a domain around which the crossover from the $t^{1/3}$ growth to the t^1 growth occurs. Here it should be noted that R_0 is known to be an increasing function of η [35,36]. On the other hand, the characteristic diffusion time for the domain size R is given by $\tau_D \sim R^2/D$, where D is the diffusion constant and $D = k_BT/(5\pi\eta\xi)$ (k_B: Boltzmann's constant). Thus, the ratio between τ_h and τ_D is given by $\tau_h/\tau_D = D\eta(R - R_0)/(k\sigma R^2)$. From the two-scale-factor universality, $\sigma = A_\sigma k_BT/\xi^2$, where A_σ is the universal constant and $A_\sigma \sim 0.2$ in 3D [37,38]. Using this relation and the expression for D, we obtain the relation $\tau_h/\tau_D \sim \xi(R - R_0)/(5\pi A_\sigma k R^2) \sim \xi(R - R_0)/(3kR^2)$. For $\tau_h < \tau_D$ [namely, for $R^2/(R - R_0) > \xi/3k$], the concentration is different from its local-equilibrium value and the local equilibrium cannot be established. Thus, the *interface quench* is likely initiated around $\tau_h/\tau_D \sim 1$. The beginning of the *interface quench* coincides with a crossover from the diffusion regime to the hydrodynamic regime. The very initial stage of phase separation is dominated by concentration diffusion. After the formation of the sharp interface due to the nonlinear contributions of the Ginzburg-Landau Hamiltonian, the hydrodynamics starts to play a significant role in coarsening for a bicontinuous pattern. The timing of the initiation of the interface quench is dependent on the value of k and R_0. In the following, we assume R_0 is small for the sake of simplicity. For bulk phase separation ($k_b \sim 0.04$), we obtain $R_t \sim 10\xi$ (R_t: the transient domain size when the *interface quench* is initiated) or $\tau_t \sim 100$ ($\tau = t/\tau_\xi$,

where $\tau_\xi = \xi^2/D$) from the condition $\tau_h/\tau_D \sim 1$. The *interface quench* probably brings the system into a different nonequilibrium (unstable or metastable) state and thus causes the retarded, secondary phase separation.

These values of R_t/ξ and τ_t in bulk are consistent with the crossover from the slow, diffusion growth to the fast, hydrodynamic growth in the scaled plots of $2\pi R/\xi$ against τ [6–8,25]. It should be noted that there might be a slight time dependence of the interface tension σ in the initial stage, which could affect the coarsening rate ($\propto \sigma/\eta$). This effect might lead to the slowing down of the coarsening and accordingly weaken the interface quench effect.

With an increase in η, R_t becomes larger, reflecting an increase in R_0 with η. This is also related to the phenomenon which is known as the N-branching effect for polymer blends [35]. For large η, therefore, R_t could become more than 100ξ. In such a case, δT is so small since the concentration $\Delta\phi_l$ is so close to the final equilibrium one and, thus, we cannot expect any significant effect of the *interface quench*. This is consistent with the fact that with an increase in η, the decay length of velocity field becomes shorter and the hydrodynamic effect becomes weaker. Thus, the behavior in a fluid system probably becomes more similar to that in a solid system with an increase in η.

3. Rate of interface quench

Next, we estimate the rate of the *interface quench*, which should likely be large enough to cause the secondary phase separation. For $\Delta\phi_t > \Delta\phi_s$, the secondary phase separation probably occurs in a metastable region or in a transitional region between an unstable and a metastable state [18]. For $\Delta\phi_t < \Delta\phi_s$, on the other hand, it occurs in an unstable region. Here, we consider the equivalent temperature quench given by Eq. (10). The quench rate around $R \sim R_t$ is estimated from

$$\frac{\partial \Delta T_t}{\partial t} = \frac{\xi}{\beta}\Delta T R_t^{-2}\left(1-\frac{2\xi}{R_t}\right)^{(-1+1/2\beta)}\frac{k\sigma}{\eta} \sim \frac{5\pi k A_\sigma}{\beta}(\Delta T/(R_t^2/D)). \quad (11)$$

For $R_t \sim 10\xi$, $\partial\Delta T_t/\partial t = 4\times 10^{-3}\Delta T/(\xi^2/D)$. For an isobutyric acid-water (IW) mixture, for example, $\xi^2/D \sim 2\times 10^{-10}(\Delta T/T_c)^{-3\nu}$ [39,40]. Thus, the initial quench rate is 0.7 mK/s for $\Delta T = 10$ mK and 400 K/s for $\Delta T = 1$ K. Further, the average quench rate from $R_t = 10\xi$ to $R = 100\xi$ can also be estimated as

$$\frac{\delta T}{\delta t} = \frac{0.3\Delta T}{90\xi}\frac{k\sigma}{\eta} = 4\times 10^{-4}\Delta T/(\xi^2/D). \quad (12)$$

The average quench rate is practically more important than the initial quench rate. For an IW mixture, the average quench rate is 0.07 mK/s for $\Delta T = 0.01$ K and 40 K/s for $\Delta T = 1$ K. The former rate is probably too slow to cause double phase separation, while the latter rate is probably fast enough. There is probably a threshold between them to cause secondary phase separation, especially in the metastable region. It should be noted that for polymer mixtures including polymer solutions, the bare correlation length ξ_0 is large even for large ΔT and, thus, the quench rate is significantly smaller in polymer mixtures than in binary liquid mixtures. Generally, the *interface quench* effect is more significant for larger σ, smaller ξ_0, smaller η, or larger ΔT. As estimated above, the quench rate steeply increases with an increase in the quench depth ΔT. This is qualitatively consistent with our experimental finding that the double phase separation was observed only for large ΔT.

4. Flow effect on secondary phase separation

Here, we briefly consider the effects of a shear in the Poiseuille flow inside a bicontinuous tube, which might suppress the secondary phase separation. The characteristic shear rate S is estimated as $S \sim \sigma/(\eta R) \sim t^{-1}$. Since $S\tau_\xi \sim \tau_\xi/t = \tau^{-1}$ is less than 0.01 for $\tau > 100$, the system is in a very weak shear regime. The effect of shear becomes weaker with the phase-separation time. The retardation of the appearance of the secondary phase separation could be caused by the crossover between the suppression effect of shear and the thermodynamic instability. The shear stress ηS breaks the droplet having a size more than $R_c \sim k\sigma/(\eta S)$, for which the shear stress exceeds the capillary pressure ($\sim \sigma/R$). Thus, when the critical radius $r_c(\sim \xi/\phi)$ is smaller than R_c, nucleation is allowed [41]. This condition can be rewritten as $S\tau_\xi < \phi_m$ (ϕ_m: the volume fraction of the minority phase in the second phase separation). ϕ_m can be estimated as

$$\phi_m = \frac{1}{2}\left(1-\frac{\Delta\phi_t}{\Delta\phi_b}\right) = \frac{1}{2}\left[1-\left(1-\frac{2\xi}{R_t}\right)^{1/2}\right]. \quad (13)$$

For $R_t \sim 10\xi$, $\phi_m \sim 0.05$. Thus, the condition $S\tau_\xi < \phi_m$ is satisfied in the late stage (for a large τ) and the nucleation could be allowed. As pointed out by Onuki [41], however, since the birth process of the critical nucleus remains unknown, the nucleation under shear need further study.

5. Double phase separation induced by interface quench

To observe a retarded phase separation, the phase separation has to proceed considerably within τ_D. Otherwise, the deviation of the concentration from its local equilibrium value will be removed by diffusion. Thus, at least one of the two phases is likely required to become unstable for an *interface quench*, since in a metastable state the metastability might be removed by the concentration diffusion during the incubation time. This requirement likely determines a certain threshold for an *interface quench* to cause a secondary, phase separation. Actually, a certain level of the quench depth ΔT is necessary to cause the double phase separation as described in Sec. III and also in Ref. [10]. Figure 14 shows the

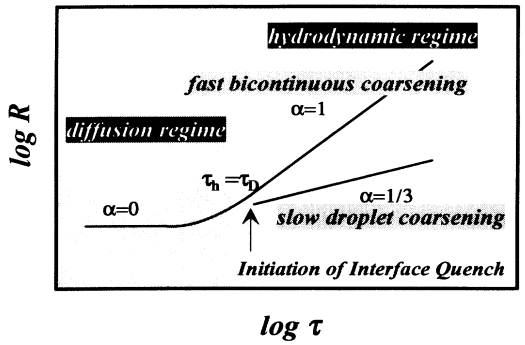

FIG. 14. A schematic figure for the coarsening process of DPS. Around $\tau_D = \tau_h$, there is a gradual transition from the diffusion regime to hydrodynamic regime, which leads to spontaneous, secondary phase separation. Here, α is the time exponent of the scaling relation $R \sim t^{\alpha}$.

relation between the main phase separation and the secondary phase separation caused by the *interface quench effect*, focusing on the coarsening dynamics. The secondary phase separation is likely spontaneously triggered around the time where $\tau_h \sim \tau_D$. This behavior is consistent with the results of light-scattering experiments by Wiltzius and Cumming [23], although these experiments were made in a confined geometry. The difference between the fast hydrodynamics coarsening ($R \sim t$ or $t^{3/2}$ [9,19,23]) and the slow droplet coarsening ($R \sim t^{1/3}$) is the main reason why the secondary phase separation apparently looks retarded from the main phase separation for microscopic observation (see Fig. 14). For understanding this phenomena more deeply, it is a prerequisite to solve Eqs. (1)–(3) without any assumptions.

B. Interface quench under an influence of wetting: anisotropic domain coarsening and ordering

For bicontinuous phase separation under an influence of wetting, Wiltzius and Cumming [23] found that the size of the wetting droplet l grows as $t^{3/2}$ although the growth mechanism was not clear. We have recently explained this anomalous, fast growth mode found by them as follows [9,19]. There is a pressure gradient between a bicontinuous tube and its wetting part, reflecting the difference in the transverse curvature of the tube between them. Thus, there should be a hydrodynamic flow from a tube to a wetting droplet spreading on the wall. Since the pressure gradient between the tube and the wetting layer is $\sim \sigma/R$ over the distance R, the flux of this flow is estimated as $Q \sim (\sigma/\eta)R^2$, where η is the viscosity and R is the characteristic size of the tube. Here, we assume that the droplet growing along the surface has a disklike shape with a thickness of h and the growth (spreading process) is almost two dimensional, or h =const. This assumption is probably valid in the case of *strong wettability* since there, the driving force of spreading is to gain the wetting energy $\Delta\gamma(=\gamma_\alpha - \gamma_\beta, \gamma_i$: the surface interaction energy for i phase). In other words, for strong wettability the solid-surface energy $\Delta\gamma$ is likely more important than the liquid-liquid interfacial energy σ. This 2D nature of the droplet growth has been experimentally confirmed [23]. In this situation, the limiting process of the droplet spreading is likely the supply of the more wettable phase from the tubes by the hydrodynamic flow, and, thus, we get the relation $ldl/dt \sim Q$. Using the Siggia's growth law for the bulk, $R \propto (\sigma/\eta)t$, we obtain the relation $l \sim [(\sigma/\eta)t]^{3/2}$. This is consistent with their observation. The prefactor $(\sigma/\eta)^{3/2}$ is roughly proportional to $(\Delta T)^{3\nu}$, where ΔT is the quench depth, ν is the critical exponent for the correlation length ξ, and $\nu \sim 0.63$ for the 3D Ising model. This dependence of the prefactor on ΔT seems to be consistent with the experimental results [23].

For a weak wetting case, on the other hand, the droplet spreading might not be purely two dimensional. When the droplet spreading is mostly dominated by hydrodynamics and the solid-surface effect does not play a dominant role in spreading, the droplet growth likely becomes three dimensional. For a three-dimensional droplet growth ($h = l$), for instance, we obtain $l^2 dl/dt \sim Q$. Thus, we can obtain the general relation $l \sim [(\sigma/\eta)t]^{3/d}$, where d is the spatial dimensionality of wetting droplet. For half-spherical droplet growth ($d = 3$) $l \sim t$, while for disklike droplet growth ($d = 2$) $l \sim t^{3/2}$. The transitional behavior of the exponent from 1 to 3/2 observed by Shi *et al.* [42] could be explained as above.

It should be noted that Troian [26] proposed another mechanism on this fast growth mode. Although this model itself is interesting, we believe that the hydrodynamic coarsening is likely responsible for this unusually fast coarsening. Probably, any mechanism based on diffusion mechanisms [26] cannot explain such a quick coarsening.

This fast coarsening ($R \sim t^{3/2}$), which is driven by wettability, results in the quick reduction of the total interfacial area between the two separated phases. Even for a weak wettability case, where $R = k_w(\sigma/\eta)t$ (k_w: the prefactor for bicontinuous phase separation affected by wetting), k_w (~ 0.1) is larger than k_b (~ 0.04). Thus, the interface quench effect under an influence of wetting is expected to be much more significant than that in bulk. For example, $R_t \sim 3\xi$ for $k_w \sim 0.1$ and R_t is smaller for phase separation under the influence of wetting than for bulk phase separation. For a strong wettability case, the effective quench rate is much larger because of the larger time exponent of the domain growth ($R \sim t^{3/2}$), in addition to a smaller R_t compared to bulk phase separation.

In 1D capillary experiments, for example, we have observed that the separation into the macroscopic phases has been accomplished within about a second after the temperature quench [17] (see, also, Figs. 2, 3, and 4). Namely, most of the bicontinuous interface whose total area is quite large in the beginning of phase separation suddenly disappears within a few seconds. If we assume that the hydrodynamic coarsening starts to play a role around $R \sim 5\xi$, the equivalent temperature quench depth is approximately $0.5\Delta T$ for the quench depth ΔT and, thus, the quench rate is ~ 0.5 K/s for $\Delta T = 1$ K. These quench depth and quench rate are likely enough to cause

a spontaneous double phase separation [22]. This is quite consistent with our observation.

C. Relation between interface quench effect proposed here and numerical study of phase-separating binary fluids by Shinozaki and Oono

The concept of *interface quench* seems to be supported by a recent computer simulation of phase-separating binary fluids by Shinozaki and Oono [12,43], which clearly shows that the concentration does not reach the final equilibrium one even after the formation of a sharp interface for a hydrodynamic system having small viscosity.

Recently, Shinozaki [43] has presented a numerical study of the dispersion relation for the linearized operator about the interfacial wall solution to a model of spinodal decomposition of an incompressible binary fluid. The results are, further, compared with computer simulation of phase-separating binary fluids by Shinozaki and Oono [12]. It has been shown that the bottom of the essential spectrum behaves like $\omega \sim k^2$, where k is a wave number along the interface and ω is the angular frequency ($\omega \sim t^{-1}$). The dispersion relation $\omega \sim k^2$ for the bottom of the essential spectrum is suggestive of bulk diffusion. On the other hand, the Nambu-Goldstone (NG)-like mode which describes the translational motion of an interface has the form of $k \sim \omega^{1/3}$ for short time (small ω^{-1}) and of $k \sim \omega$ for long time (large ω^{-1}). This is consistent with the well-known coarsening law for symmetric fluid mixtures ($R \sim t^{1/3}$ for small t and $R \sim t$ for large t) [1]. It is found by them that (i) the NG branch hits the essential spectrum before it reaches the asymptotic behavior of $k \sim \omega$ for small η and (ii) for large η the NG branch already behaves like $k \sim \omega$ when it hits the essential spectrum. The behavior can be seen, for example, in Fig. 62 of Ref. [12]. Their results indicate that the diffusion time scale ($\sim R(t)^2$) is much longer than the time scale of hydrodynamic growth ($\sim R(t)$), which is quite consistent with our prediction [9,10].

They mentioned that numerical instability empirically occurs at the point in the simulation when the essential spectrum crosses the NG dispersion relation before the latter reaches the asymptotic behavior of $k \sim \omega$. We think that this fact is likely closely related to our "*double phase separation*" spontaneously caused by the *interface quench* effect. Numerical instability might reflect the thermodynamic metastability or instability of phases. Further studies on numerical instability focusing on whether the instability is intrinsic or caused by the problem of calculation techniques are highly desirable.

VII. SUMMARY

In summary, we demonstrate that the hydrodynamic *interface quench* effects could play significant roles in both surface-mediated and bulk bicontinuous spinodal decomposition. The effects are caused by a strong coupling between the concentration and the velocity fields which violates the local equilibrium. The *interface quench* effects could cause double phase separation for bicontinuous phase separation. We found experimental evidence of the *interface quench effect*, namely, double phase separation, under a geometrical constraint, where a wetting effect further accelerates the hydrodynamic coarsening. This effect should affect the pattern formation dynamics and the morphology significantly. Experimentally it is important to check the possibility of spontaneous, double phase separation in bulk. Further, it is necessary to completely rule out the possibility that double phase separation is caused by a thermal history effect, although this possibility is probably very low as discussed in Sec. IV C. We think that the *interface quench* has at least conceptual importance even for bulk phase separation. The phenomena described here should be universal for any binary fluid mixtures. Since the discussion here is rather of qualitative nature, we need further theoretical studies on the mechanisms proposed here to establish the concept of *the self-induced interface quench*, including the estimation of the coarsening rate. Computer simulation [12,36,43] could provide us with key information on this problem. The local-equilibrium assumption has so far been believed to be valid in the late stage of phase separation, however, this study indicates that it is not necessarily valid for nearly symmetric mixtures where the concentration field can strongly be coupled with the velocity field.

Noted added in proof. After the submission of this paper, the author became aware of the work by Perrot *et al.* [F. Perrot, P. Guenoun, T. Baumberger, and D. Beysens, Phys. Rev. Lett. **73**, 688 (1994)]. They also pointed out that droplet phase separation is observed in a wider composition region and attributed it to the regular droplet distribution, similar to our discussion in Sec. II.

ACKNOWLEDGMENTS

The author is grateful to Y. Oono and A. Shinozaki for providing useful information. This work was partly supported by a Grant-in-Aid from the Ministry of Education, Science, and Culture, Japan and also by a grant from the Ciba-Geigy Foundation (Japan) for the Promotion of Science.

[1] J.D. Gunton, M. San Miguel, and P. Sahni, in *Phase Separation and Critical Phenomena*, edited by C. Domb and J.H. Lebowitz (Academic, London, 1983), Vol. 8.

[2] *Dynamics of Ordering Process in Condensed Matter*, edited by S. Komura and H. Furukawa (Plenum, New York, 1987).

[3] P.C. Hohenberg and B.I. Halperin, Rev. Mod. Phys. **49**, 435 (1976).

[4] E.D. Siggia, Phys. Rev. A **20**, 595 (1979).

[5] Y.C. Chou and W.I. Goldburg, Phys. Rev. A **20**, 2105 (1979).

[6] T. Hashimoto, M. Itakura, and N. Shimazu, J. Chem.

Phys. **85**, 6118 (1986).
[7] T. Hashimoto, M. Itakura, and H. Hasegawa, J. Chem. Phys. **85**, 6773 (1986).
[8] F.S. Bates and P. Wiltzius, J. Chem. Phys. **91**, 3258 (1989).
[9] H. Tanaka, in *Ordering in Macromolecular Systems*, edited by A. Teramoto, M. Kobayashi, and T. Norisuye, Proceedings of the Osaka University Macromolecular Symposium OUMS (Springer-Verlag, Berlin, 1994), p. 291.
[10] H. Tanaka, Phys. Rev. Lett. **72**, 3690 (1994).
[11] H.Tanaka, Phys. Rev. Lett. **72**, 1702 (1994).
[12] A. Shinozaki and Y. Oono, Phys. Rev. E **48**, 2622 (1993).
[13] H. Tanaka, Macromolecules **25**, 6377 (1992).
[14] H. Tanaka, Phys. Rev. Lett. **71**, 3158 (1993).
[15] H.Tanaka, J. Chem. Phys. **100**, 5323 (1994).
[16] H. Tanaka and T. Nishi, Phys. Rev. Lett. **59**, 692 (1987).
[17] H. Tanaka, Phys. Rev. Lett. **70**, 53 (1993).
[18] H. Tanaka, T. Yokokawa, H. Abe, T. Hayashi, and T. Nishi, Phys. Rev. Lett. **65**, 3136 (1990).
[19] H. Tanaka, Phys. Rev. Lett. **70**, 2770 (1993).
[20] J. Bodensohn and W.I. Goldburg, Phys. Rev. A **46**, 5084 (1992).
[21] H. Tanaka, Europhys. Lett. **24**, 665 (1993).
[22] H. Tanaka, Phys. Rev. E **47**, 2946 (1993).
[23] P. Wiltzius and A. Cumming, Phys. Rev. Lett. **66**, 3000 (1991).
[24] A. Cumming, P. Wiltzius, F.S. Bates, and J.H. Rosedale, Phys. Rev. A **45**, 885 (1992).
[25] P. Guenoun, R. Gastaud, F. Perrot, and D. Beysens, Phys. Rev. A **36**, 4876 (1987), in Ref. 2.
[26] S.M. Troian, Phys. Rev. Lett. **71**, 1399 (1993).
[27] J.F. Marko, Phys. Rev. E **48**, 2861 (1993).
[28] N.C. Wong and C.M. Knobler, Phys. Rev. A **24**, 3205 (1981).
[29] It should be noted that even in a strong geometrical confinement a double temperature quench is confirmed to cause double phase separation. Thus, the suppression of double phase separation in a strong confinement cannot be explained by thermal history effects.
[30] K. Kawasaki and T. Ohta, Physica A **118**, 175 (1983).
[31] V.G. Levich, *Physicochemical Hydrodynamics* (Prentice-Hall, Englewood Cliffs, N.J., 1962).
[32] N.C. Wong and C.M. Knobler, J. Chem. Phys. **69**, 725 (1978).
[33] M. San Miguel, M. Grant, and J.D. Gunton, Phys. Rev. A **31**, 1001 (1985).
[34] The trapezoidal profile is probably a good approximation in the late stage [$\tau = t/(\xi^2/D) \geq 200$] [8], and this assumption will not affect the main conclusion.
[35] A. Onuki, J. Chem. Phys. **85**, 1122 (1986).
[36] T. Koga and K. Kawasaki, Physica A **196**, 389 (1993).
[37] G. Howland, N.C. Wong, and C.M. Knobler, J. Chem. Phys. **73**, 522 (1980).
[38] H. Chaar, M.R. Moldover, and J.W. Shmidt, J. Chem. Phys. **85**, 418 (1986).
[39] B. Chu, F.J. Schoenes, and W.I. Kao, J. Am. Chem. Soc. **90**, 3402 (1968).
[40] E. Gulari, A.F. Collings, R.L. Schmidt, and C.J. Pings, J. Chem. Phys. **56**, 6169 (1972).
[41] A. Onuki, Phys. Rev.A **34**, 3528 (1993).
[42] B.Q. Shi, C. Harrison, and A. Cumming, Phys. Rev. Lett. **70**, 206 (1993).
[43] A. Shinozaki, Phys. Rev. E **48**, 1984 (1993).

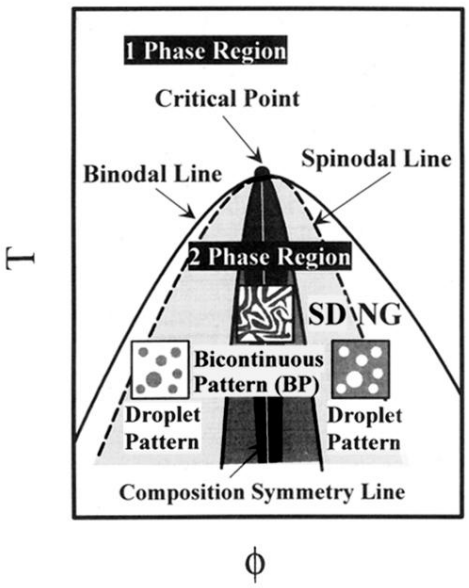

FIG. 1. A schematic phase diagram of a binary fluid mixture. The two-phase region is divided into metastable and unstable regions. In the former nucleation-growth-type phase separation (NG) occurs, while in the latter spinodal-decomposition-type phase separation (SD) occurs. From the morphological viewpoints, further, an unstable, spinodal region can be grouped into the two regions corresponding to bicontinuous phase separation and droplet phase separation, depending upon the composition symmetry. Here, we assume that the two components are dynamically symmetric for the sake of simplicity. The coarsening dynamics is closely correlated with the morphology. Any asymmetry breaks a bicontinuous structure and at a certain time there is a transition from a bicontinuous to droplet morphology. In the figure, the two bicontinuous regions are drawn for two different phase-separation times. The brighter region is for the earlier stage of phase separation, while the darker region is for the later stage.

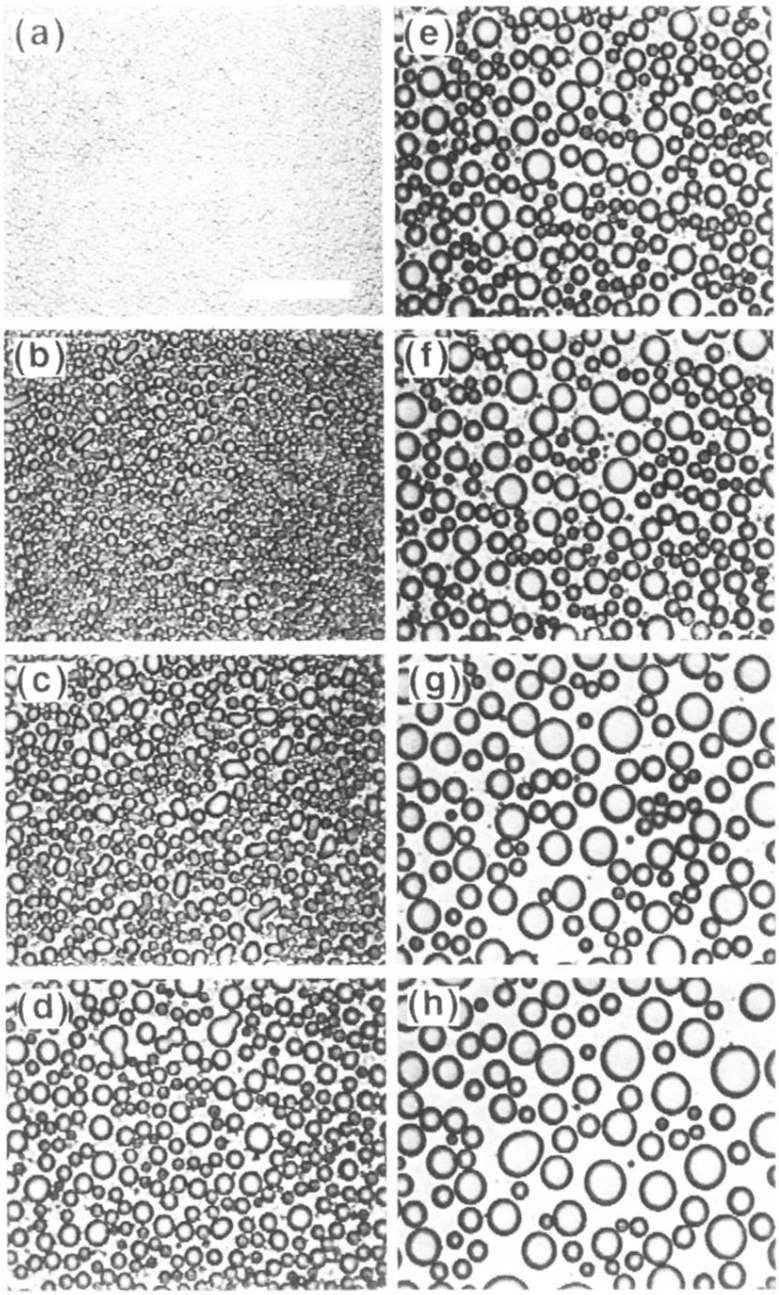

FIG. 10. Phase separation in a 2D capillary for OCL-OS (5:5) at 60 °C. The quench depth and the quench rate are the same as those in Fig. 8. The sample thickness d is about 8 μm. (a) 5 s, (b) 10 s, (c) 20 s, (d) 60 s, (e) 240 s, (f) 540 s, (g) 1740 s, (h) 2940 s after the quench. Here, there is no indication of secondary phase separation. The bar corresponds to 100 μm.

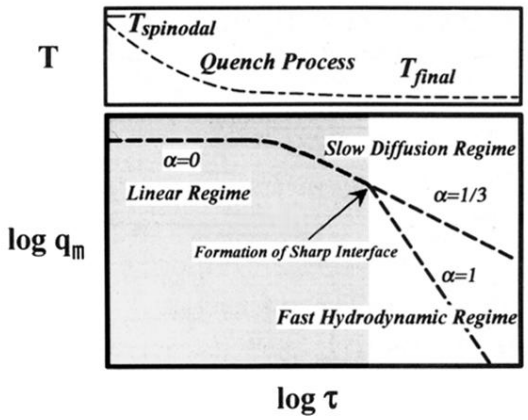

FIG. 12. A schematic figure of the coarsening behavior for both bicontinuous and droplet phase separation. In both cases, diffusion dominates the coarsening behavior until the formation of a sharp interface. The shaded region is the time regime dominated by concentration diffusion. Here, α is the time exponent of the scaling relation $q_m \sim t^{-\alpha}$. If the transient process of a temperature quench is localized only in the shaded region, the thermal history effects should affect the phase separation in the same way for both types of phase separation.

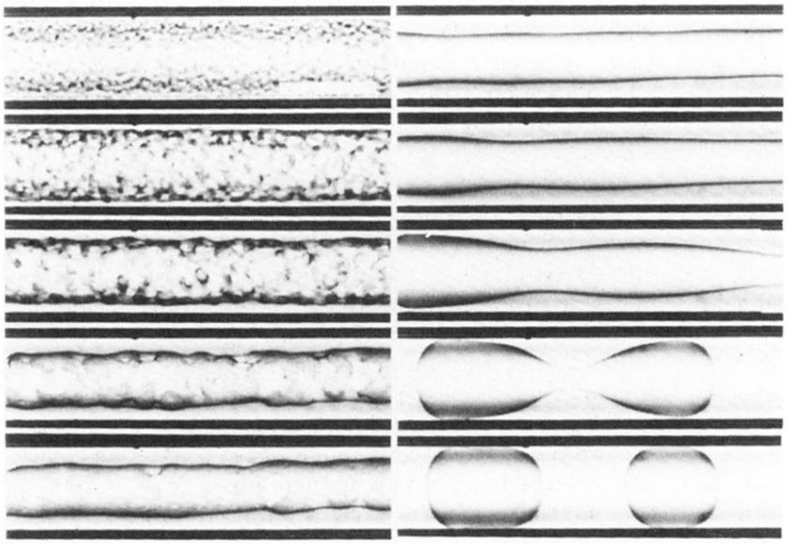

FIG. 2. Phase separation in a 1D capillary for PVME-water (7:93). Photographs correspond to 1.0 s, 1.5 s, 2.0 s, 3.0 s, 4.0 s (left column); 17.0 s, 57.0 s, 87.0 s, 127.0 s, 147.0 s (right column); from top to bottom, respectively, after the temperature jump from 32.5 °C to 33.5 °C. The bar corresponds to 200 μm.

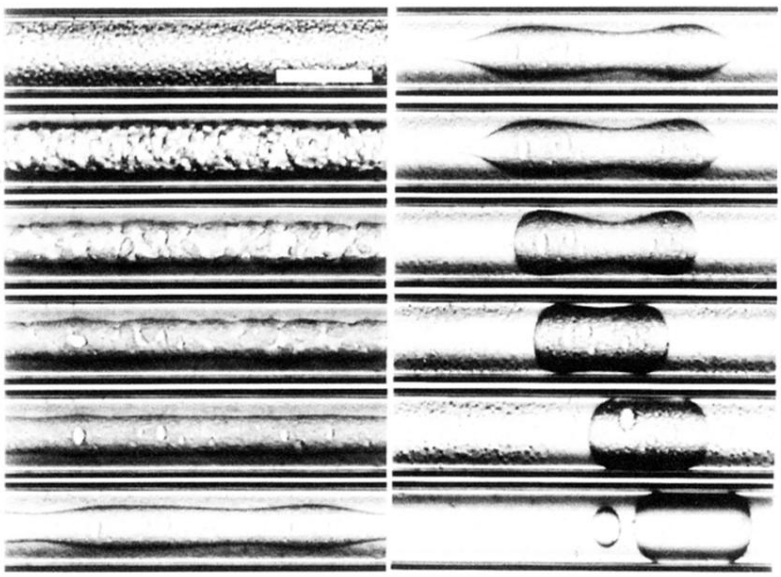

FIG. 3. Phase separation in a 1D capillary for PVME-water (7:93) mixture. Photographs correspond to 0.3 s, 0.8 s, 1.3 s, 1.8 s, 3.8 s, 16.8 s (left column); 22.3 s, 23.8 s, 28.8 s, 88.8 s, 479.0 s, and 3000 s (right column); from top to bottom, respectively, after the temperature jump from 32.5 °C to 34.0 °C. The bar corresponds to 200 μm.

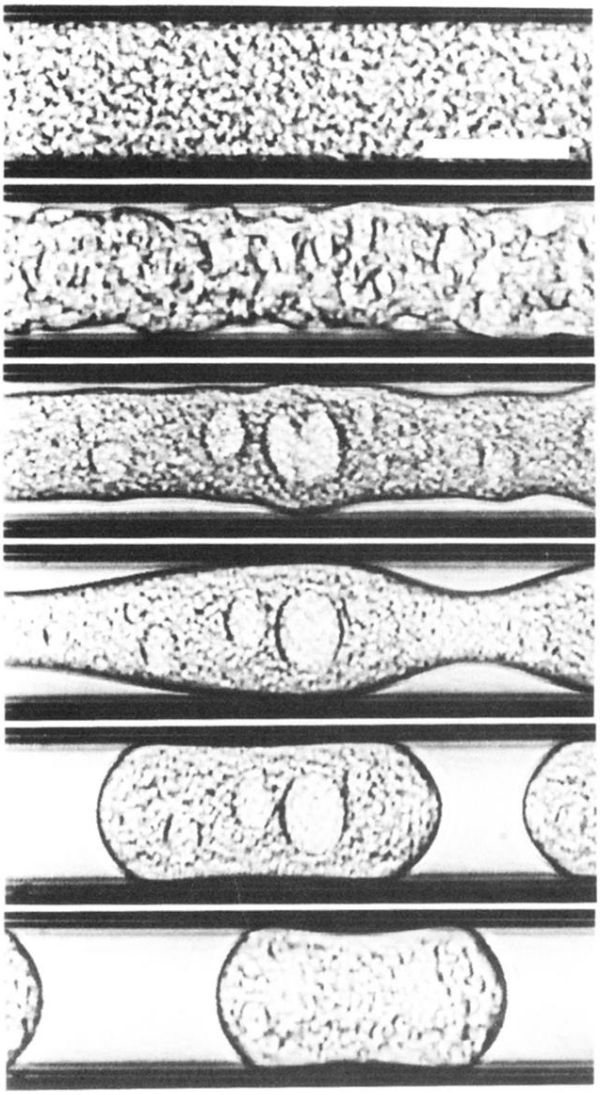

FIG. 4. Phase separation in a 1D capillary for PVME-water (10:90). Photographs correspond to 0.5 s, 1.0 s, 2.0 s, 18.0 s, 28.0 s, and 238.0 s, from top to bottom, respectively, after the temperature jump from 32.5 °C to 34.1 °C. The bar corresponds to 80 μm. In this case, the composition slightly deviates from the symmetric one (7:93). Double phase separation is selectively observed only in the polymer-rich (less-wettable) phase.

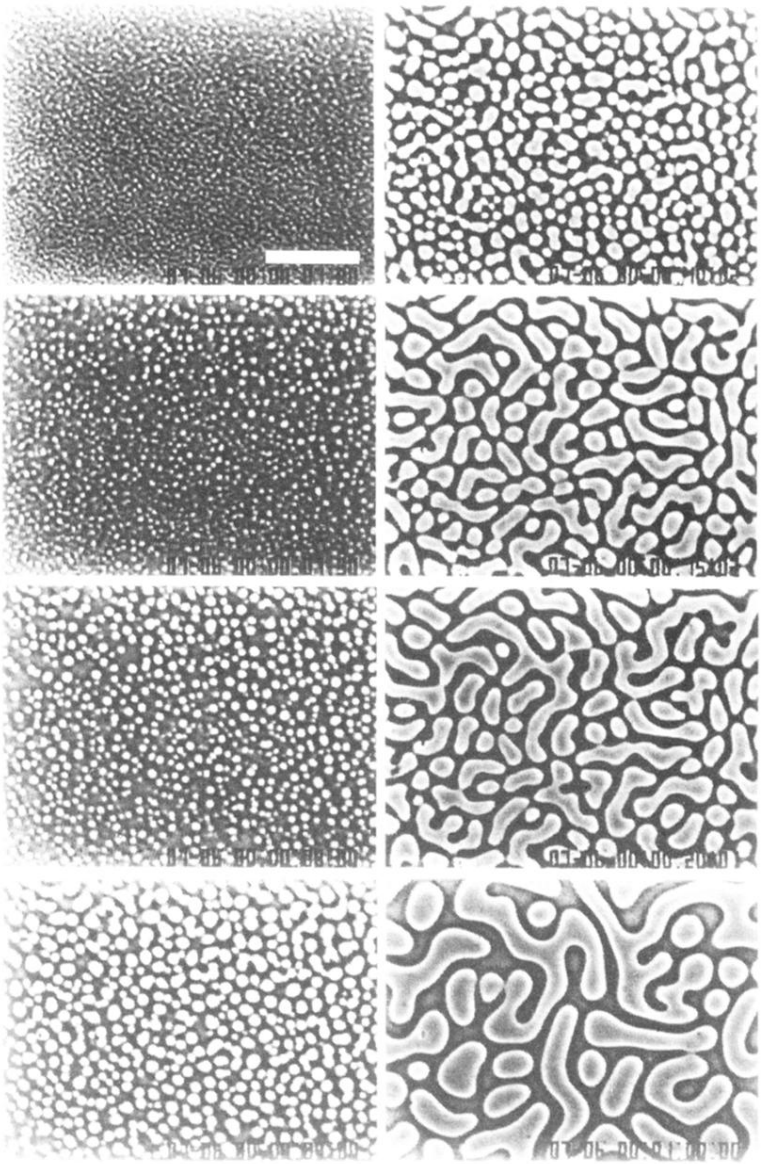

FIG. 5. Phase separation in a 2D capillary ($d \sim 3$ μm) for PVME-water (7:93). Photographs correspond to 1 s, 1.5 s, 2 s, 3 s (left column); 4 s, 9 s, 14 s, and 54 s (right column); from top to bottom, respectively, after the temperature jump from 32.5 °C to 33.3 °C. The bar corresponds to 80 μm.

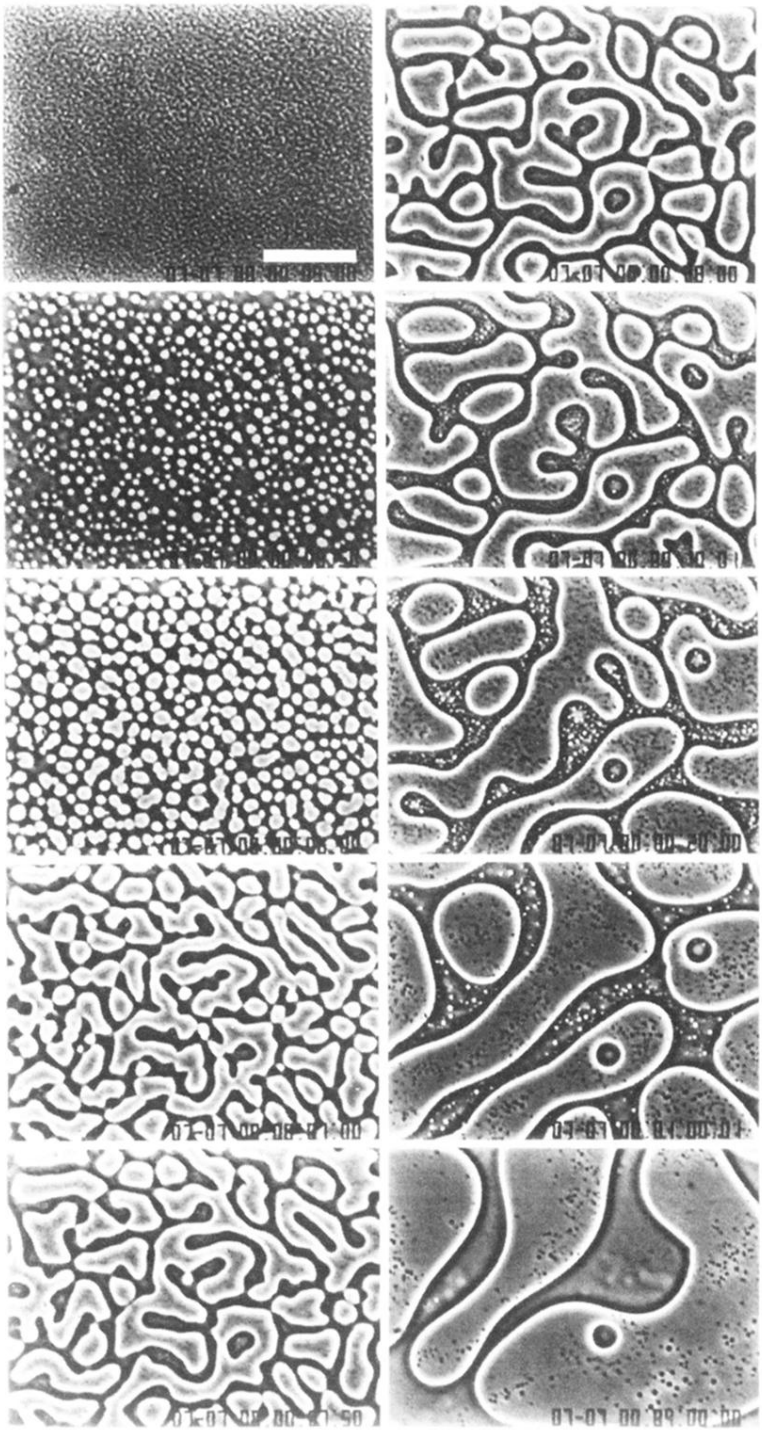

FIG. 6. Phase separation in a 2D capillary ($d \sim 3$ μm) for PVME-water (7:93). Photographs correspond to 0.2 s, 0.7 s, 1.2 s, 2.2 s, 2.7 s (left column); 3.2 s, 5.2 s, 15.2 s, 55 s, and 235 s (right column); from top to bottom, respectively, after the temperature jump from 32.5 °C to 34.0 °C. The bar corresponds to 80 μm.

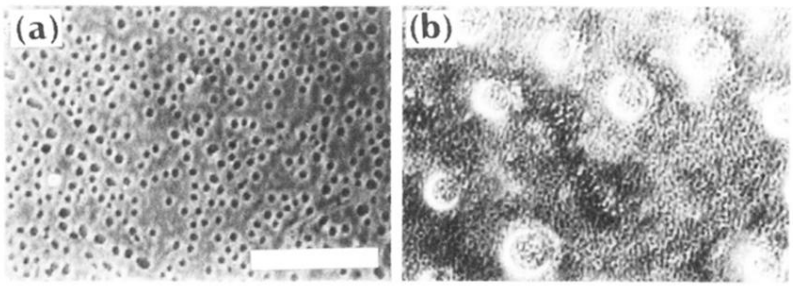

FIG. 7. Phase-separation behavior in a 2D capillary for PVME-water (7:93) at 34.0 °C. Both photographs were taken at 20 s after the temperature jump from 32.5 °C to 34.0 °C. (a) $d \sim 1$ μm, (b) $d = 15$ μm. In (b), the coexistence of large and small domains is seen, while not in (a). The bar corresponds to 100 μm.

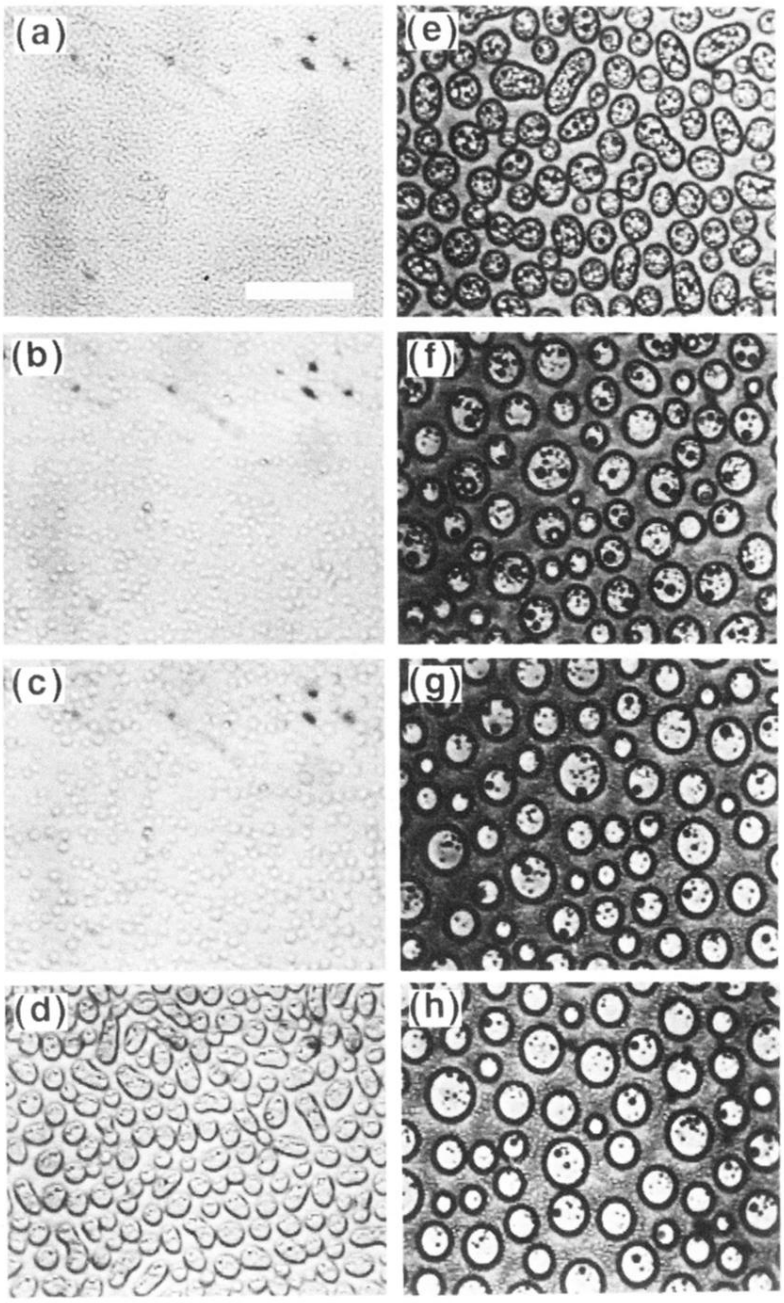

FIG. 8. Double phase separation observed in an OCL-OS (3:7) mixture at 60 °C. We can clearly see the secondary phase separation. The sample thickness d is about 8 μm. (a) 0.8 s, (b) 1.2 s, (c) 1.4 s, (d) 2 s, (e) 6 s, (f) 111 s, (g) 590 s, (h) 1200 s after the quench. The bar corresponds to 100 μm.

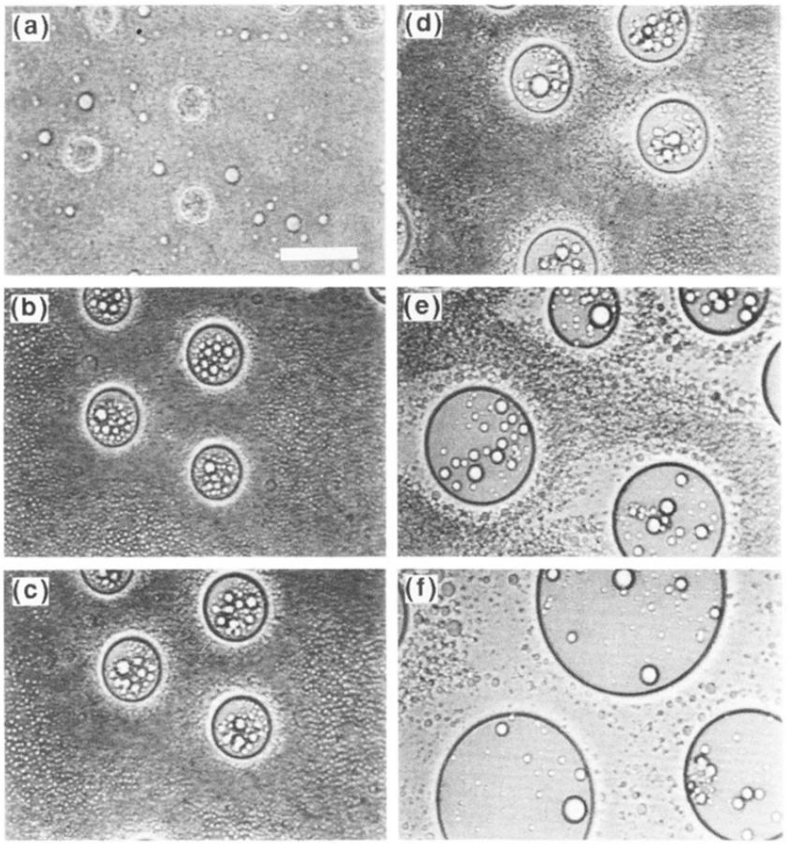

FIG. 9. Double phase separation observed in OCL-OS (3:7) at 100 ° C. We can clearly see the secondary phase separation. The sample thickness d is about 53 μm. (a) 7 s, (b) 21 s, (c) 39 s, (d) 64 s, (e) 183 s, (f) 603 s after the quench. The bar corresponds to 100 μm.